



Thermoresponsive and co-nonsolvency behavior of poly(*N*-vinyl isobutyramide) and poly(*N*-isopropyl methacrylamide) as poly(*N*-isopropyl acrylamide) analogs in aqueous media

Cristiane Henschel¹ · Dirk Schanzenbach¹ · André Laschewsky^{1,2} · Chia-Hsin Ko³ · Christine M. Papadakis³ · Peter Müller-Buschbaum^{4,5}

Received: 7 February 2023 / Revised: 28 February 2023 / Accepted: 1 March 2023 / Published online: 31 March 2023
© The Author(s) 2023

Abstract

Sets of the nonionic polymers poly(*N*-vinyl isobutyramide) (pNVIBAm) and poly(*N*-isopropyl methacrylamide) (pNIPMAm) are synthesized by radical polymerization covering the molar mass range from about 20,000 to 150,000 kg mol⁻¹, and their thermoresponsive and solvent-responsive behaviors in aqueous solution are studied. Both polymers feature a lower critical solution temperature (LCST) apparently of the rare so-called type II, as characteristic for their well-studied analogue poly(*N*-isopropyl acrylamide) (pNIPAm). Moreover, in analogy to pNIPAm, both polymers exhibit co-nonsolvency behavior in mixtures of water with several co-solvents, including short-chain alcohols as well as a range of polar aprotic solvents. While the cloud points of the aqueous solutions are a few degrees higher than those for pNIPAm and increase in the order pNIPAm < pNVIBAm < pNIPMAm, the co-nonsolvency behavior becomes less pronounced in the order pNIPAm > pNVIBAm > pNIPMAm. Exceptionally, pNIPMAm does not show co-nonsolvency in mixtures of water and *N,N*-dimethylformamide.

Keywords Phase transition · Thermoresponsive polymers · Poly(*N*-vinyl isobutyramide) · Poly(*N*-isopropyl methacrylamide) · Lower critical solution temperature · Co-nonsolvency

Introduction

The interest in the thermoresponsive behavior of polymers in aqueous solution has been mostly focused on the occurrence of a lower critical solution temperature (LCST) and

a miscibility gap at elevated temperatures, implying a coil-to-globule transition of the solvated polymer chain when passing the phase boundary [1–3]. In fact, LCST behavior is widespread among nonionic polymers in aqueous solution [4, 5]. The precise transition temperature of a given system depends on a number of molecular features, first of all on the chemical structure of the monomer and the resulting constitutional repeat unit (CRU) [4, 6, 7], or in the case of statistical copolymers, on their composition [8–12]. Moreover, it is modulated by various additional molecular parameters, such as the polymer molar mass, end groups [13, 14], and tacticity [15–17]. Further, the transition temperature depends on numerous physical parameters of the system studied, including the polymer concentration or the pressure [18–21], and can be modulated by the presence of low molar mass additives, such as electrolytes, H-bond modifiers, osmolytes, or organic co-solvents [22–25].

While numerous nonionic water-soluble polymers exhibit a lower consolute boundary with a LCST in aqueous systems, on a closer view, type I and type II LCST behaviors can be distinguished [26, 27]. The former is the standard

✉ André Laschewsky
laschews@uni-potsdam.de

¹ Institute of Chemistry, University of Potsdam, Karl-Liebknecht-Straße 24-25, Golm 14476, Potsdam, Germany

² Fraunhofer-Institute for Applied Polymer Research (IAP), Geiselbergstraße 69, Golm 14476, Potsdam, Germany

³ Soft Matter Physics Group, Department of Physics, TUM School of Natural Sciences, Technical University of Munich, James-Frank-Straße 1, 85748 Garching, Germany

⁴ Chair of Functional Materials, Department of Physics, TUM School of Natural Sciences, Technical University of Munich, James-Frank-Straße 1, 85748 Garching, Germany

⁵ Heinz Maier-Leibnitz Zentrum (MLZ), Technical University of Munich, Lichtenbergstr. 1, 85748 Garching, Germany

case and characterized by Flory–Huggins-like phase behavior, for which, e.g., the phase transition temperature changes sensitively with the polymer's concentration and molar mass. Characteristically, the polymer concentration of the critical point approaches the value of 0 with increasing molar mass. When heating across the transition temperature, such polymers undergo a marked, but continuous desolvation, or a gradual shrinking in the case of hydrogels. Type I behavior is advantageous, for instance, for applications where the LCST transition is translated into quantitative signals or effects, which change markedly, though continuously within a certain temperature interval. This behavior is typically aspired for, e.g., sensors or molecular thermometers [28–32]. A characteristic feature of the exceptional type II behavior is the existence of an off-zero liquid–liquid critical composition for a hypothetical polymer of infinite molar mass [27, 33, 34]. This means that even at high molar masses, the polymer concentration at the critical point approaches a fixed value, but does not become zero. Typically, the phase transition temperature changes only weakly with the polymer's molar mass when exceeding a value of about 20 kDa, and with its concentration over a large concentration range [35]. When heating beyond the transition temperature, such polymers undergo a rather abrupt desolvation or shrinking [26, 27], while gels show a discontinuous swelling transition [36, 37]. These features are typically advantageous for applications where the LCST transition is to be translated into a threshold value, as, e.g., for switches, actuators, valves, alarming devices, or controlled delivery purposes [38–44].

The prototype of polymers with LCST type II behavior in aqueous media is poly(*N*-isopropyl acrylamide) (pNIPAm), in which LCST is conveniently located around 30 °C [4, 27, 45–47]. Furthermore, pNIPAm shows also a rich co-nonsolvency behavior, i.e., insolubility in specific mixtures of good solvents, namely for mixtures of water and numerous water-miscible organic solvents [48–50]. Though studied intensely since long, many open questions remain on the behavior of pNIPAm [27], including, e.g., the uniqueness of pNIPAm's behavior in solution. To clarify this aspect, we studied two chemically close analogs of pNIPAm, namely, the polymers poly(*N*-vinyl isobutyramide) (pNVIBAm) and poly(*N*-isopropyl methacrylamide) (pNIPMAm) (Fig. 1), which both share the secondary amide moiety as a hydrophilic key motif, investigating the impact of their modified molecular structures on the stimuli-responsive behavior.

The CRU of pNVIBAm represents a structural isomer of pNIPAm, with the only difference that the orientation of the amide moiety relative to the polymer backbone is inverted. Accordingly, when judging on an incremental base, both polymers pNVIBAm and pNIPAm are characterized by the identical hydrophilic–hydrophobic balance. However, literature reported an LCST value of around 40 °C for pNVIBAm [18, 51–55], contrasting with the LCST value

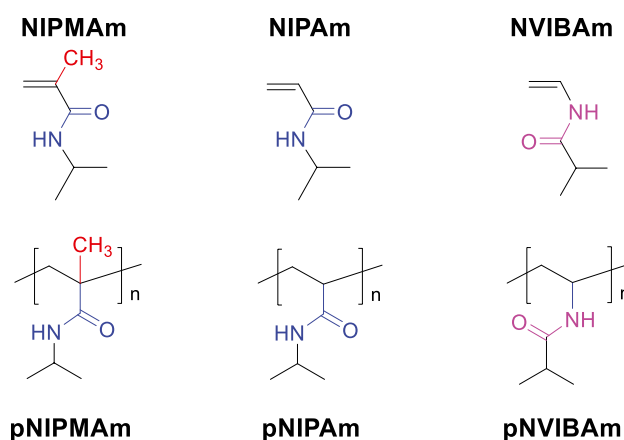


Fig. 1 Chemical structure of the polymers synthesized, poly(*N*-vinyl isobutyramide) (pNVIBAm) and poly(*N*-isopropyl methacrylamide) (pNIPMAm), in comparison to the reference poly(*N*-isopropyl acrylamide) (pNIPAm), and of their underlying monomers

of around 30 °C typically reported for pNIPAm [1, 27, 45]. The reasons for this difference are not clear so far. Anyhow, the number of reports on pNVIBAm and its phase behavior in aqueous solution is very limited, in flagrant contrast to the myriad reports on pNIPAm. Moreover, many of the few reports using NVIBAm as building block deal with chemically cross-linked hydrogels [56–58] or with copolymers [58–61], rather than with soluble homopolymers. Nevertheless, the few studies available suggest the exceptional type II LCST behavior for pNVIBAm [56] and mention, at least briefly, co-nonsolvency behavior in one system, namely in ethanol–water mixtures [62, 63].

The polymer pNIPMAm can be considered a homologue of pNIPAm bearing an additional methyl group on the polymer backbone. Although reports on pNIPMAm and its phase behavior in aqueous solution have been less rare than reports on pNVIBAm, the literature has remained quite scarce up to now, too. Notwithstanding, the structural similarity of pNIPMAm to pNIPAm has incited studies on its phase behavior in aqueous solution from the very beginning [35, 64, 65]. Remarkably, the LCST of pNIPMAm is not lower than the LCST of pNIPAm, as might have been expected due to the additional—a priori hydrophobic—methyl group of the repeat unit, but it is about 40–45 °C and thus higher [7, 64, 66–69]. Proposed explanations of this comparably high value include the sterically more crowded backbone weakening intrapolymer interactions [69–74], and an increased residence time of hydration water on the polymers [75]. Although the aqueous solution behavior of pNIPMAm shows some particularities [69, 76], it seems also to be of LCST type II [69]. Similar to pNVIBAm, only few studies mentioned co-nonsolvency behavior of pNIPMAm up to now, namely for aqueous mixtures of methanol [77], ethanol [78, 79], and acetone [44, 80].

In our study, we synthesized sets of varying molar masses for both pNVIBAm and pNIPMAm and investigated the effects of the varied molecular structures on the stimuli-responsive behavior. We studied, in particular, the phase transition temperature in pure water and in mixtures of water with a series of fully water-miscible organic solvents, comprising the protic solvents methanol, ethanol, *n*-propanol, and *iso*-propanol, as well as the aprotic solvents *N,N*-dimethylformamide (DMF), dimethylsulfoxide (DMSO), acetone, tetrahydrofuran (THF), and 1,4-dioxane.

Experimental

The chemicals and solvents used, as well as the monomer syntheses following literature procedures [81, 82], are specified in detail in the Supplementary Information.

Polymerizations

Conventional free radical polymerizations were performed to obtain pNIPMAm and pNVIBAm homopolymers. A typical procedure is presented in the following. Complete lists of all conventional free radical polymerizations along with the specific reaction parameters are provided in Tables 1 and 2.

N-Isopropyl methacrylamide (NIPMAm, 1.00 g, 7.86 mmol) was placed in a round-bottom flask equipped with a magnetic stirring bar. Initiator 2,2'-azobis(isobutyronitrile) (AIBN, 0.50 mg, 0.0031 mmol) was added, followed by additional benzene (total 2.66 mL), to achieve an overall concentration of 30 wt%. The flask was closed with a silicone septum and degassed with argon for 15 min, after which the flask was immersed in an oil bath of 65 °C. The reaction was allowed to proceed for 18 h, and then quenched by exposure to air and cooling to room temperature. The polymer was dissolved in acetone and precipitated into a

tenfold volume of 2:1 diethyl ether/pentane. The precipitate was collected by filtration, and precipitation was repeated, if necessary, until no residual monomer was present, as evidenced by ¹H NMR analysis. Finally, the polymer was dissolved in water and lyophilized to yield a colorless, hygroscopic powder.

Methods and equipment

¹H NMR and ¹³C NMR spectra were recorded at ambient temperature in deuterated solvents, using a Bruker Avance 300 (300 MHz/75 MHz), Bruker Avance NEO 400 (400 MHz/101 MHz), Bruker Avance Neo 500 (500 MHz/126 MHz), or Bruker AVANCE III (600 MHz/151 MHz) spectrometer, depending on the resolution and sensitivity needed. Polymer concentrations were around 40 g L⁻¹.

Size exclusion chromatography (SEC) of the polymers was performed at 25 °C in NMP with 0.5 wt% of LiBr added as an eluent, using a TSP P1000 isocratic pump (Thermo Fisher Scientific, Dreieich, Germany), a Shimadzu RID-6A refractive index detector (Shimadzu Corporation, Kyoto, Japan), and a PSS GRAM column (7 μm, 8 × 300 mm) (PSS GmbH, Mainz, Germany). The SEC setup was calibrated using narrowly distributed poly(methyl methacrylate) (PMMA) standards (PSS GmbH, Mainz, Germany).

Cloud points (T_{CP}) of the polymers were determined by turbidimetry using a Varian Cary 5000 UV–Vis–NIR spectrophotometer, equipped with 6 + 6 cell Peltier thermostated cell holders, using quartz cuvettes with an optical path length of 10 mm. Measurements were performed at a wavelength (λ) of 500 nm, with heating and cooling rates of 0.5 K min⁻¹. Measured transmission values were normalized to the maximum value in each sample's measurement. Cloud points were determined from the heating run, using the onset temperature of the transmission decay. Polymer solutions in mixed solvents (water + co-solvent)

Table 1 Reaction conditions and conversions of the radical solution polymerizations of NVIBAm (30 wt% monomer in benzene), and key polymer parameters of the polymers obtained

Entry	Sample	Initiator	Temp. (°C)	Duration (h)	<i>M</i> : <i>I</i> ^a	Conv. (%)	M_n^{SEC} ^b (kg mol ⁻¹)	\mathcal{D}^{SEC} ^c
1	pNVIBAM ₃₇₇	AIBN	65	5	600:1	80	43	2.1
2	pNVIBAM ₃₀₃	AIBN	65	3.5	600:1	62	34	2.0
3	pNVIBAM ₁₀₆₉	MAIB	66	1.75	800:1	78 ^d	121	2.9
4	pNVIBAM ₃₄₀	MAIB	66	5.3	850:1	56	39	1.9
5	pNVIBAM ₂₈₇	MAIB	66	4	850:1	42	32	1.8
6	pNVIBAM ₈₁	AIBN	65	16	2710:1 ^e	10	9.3	1.6

^aMolar ratio of monomer: initiator

^bThe number average molar mass by size exclusion chromatography (SEC), eluent 0.5 wt% LiBr in NMP, and calibration by narrowly distributed poly(methyl methacrylate) standards

^cDispersity index

^dYield is given in lieu of conversion

^eTen equivalents of RAFT chain transfer agent CTA-X added compared to the amount of initiator

Table 2 Reaction conditions and conversions achieved of the radical polymerization of NIPMAm in various solvents and with different azo initiators (monomer concentration 30 wt% if not stated otherwise), and key polymer parameters of the polymers obtained

Entry	Sample	Initiator	Solvent	[M]:[I] ^a	Temp. (°C)	Duration (h)	Conv. (%)	$M_n^{SEC\ b}$ (kg mol ⁻¹)	$\bar{D}^{SEC\ c}$
7	pNIPMAm ₅₁	AIBN	THF ^d	167:1	60	23	51 ^e	7	1.7
8 ^f	pNIPMAm ₁₃₃	AIBN	THF ^d	200:1	60	18	59 ^e	17	1.8
9 ^g	pNIPMAm ₉₁	AIBN	THF ^h	200:1	60	22	53 ^e	11	2.0
10	pNIPMAm ₄₉₂	AIBN	Benzene	360:1	65	18	93	63	2.6
11	pNIPMAm ₂₆₄	AIBN	Benzene ⁱ	610:1	65	24	57	34	2.1
12	pNIPMAm ₃₀₁	AIBN	Benzene ⁱ	610:1	65	24	65	38	2.1
13	pNIPMAm ₃₀₅	AIBN	Benzene ⁱ	610:1	65	24	60	39	2.0
14	pNIPMAm ₂₉₅	AIBN	Benzene ⁱ	610:1	65	24	74	37	2.2
15	pNIPMAm ₃₃₉	AIBN	Benzene ⁱ	610:1	65	24	72	43	2.1
16	pNIPMAm ₄₄₅	AIBN	Benzene ⁱ	1200:1	65	18	46	57	2.1
17	pNIPMAm ₃₉₀	AIBN	Benzene	1200:1	65	18.5	26	50	1.9
18	pNIPMAm ₃₉₃	AIBN	Benzene	1200:1	65	18	63	50	2.8
19	pNIPMAm ₇₇₆	AIBN	Benzene	1200:1	65	18	89	99	2.8
20	pNIPMAm ₉₅₆	AIBN	Benzene	1200:1	65	18	96	122	3.0
21	pNIPMAm ₄₆₉	AIBN	Benzene ^j	1200:1	72	18	79	60	2.6
22	pNIPMAm ₄₂₄	AIBN	Benzene ^j	1200:1	72	18.5	41	54	2.1
23	pNIPMAm ₄₂₆	MAIB	Benzene ⁱ	1200:1	66	18	51	54	2.5
24	pNIPMAm ₉₃₆	MAIB	Benzene	1630:1	66	18.5	54	119	2.7
25	pNIPMAm ₂₄₁	AIBN	TFE ^h	1200:1	65	18.5	89	31	2.8
26	pNIPMAm ₈₁₀	AIBAH	TFE ^h	1200:1	56	17	66	103	1.8
27	pNIPMAm ₈₉₅	AIBAH	TFE	1200:1	56	18	85	114	2.0
28	pNIPMAm ₁₁₅₄	AIBAH	TFE	1200:1	56	18	52	147	2.0
29	pNIPMAm ₂₀₁	AIBAH	TFE	1200:1	56	18.5	91	26	2.3
30	pNIPMAm ₆₈₉	AMODMV	Ethanol	1200:1	30	18	63	88	1.8
31	pNIPMAm ₂₁₉	AMODMV	Ethanol	1200:1	30	18	31	28	3.2
32	pNIPMAm ₆₈₂	AMODMV	Ethanol	1210:1	30	18	35	87	2.0
33	pNIPMAm ₃₈₁	AMODMV	Ethanol	1200:1	30	18	21	48	2.0

^aMolar ratio of monomer:initiator^bThe number average molar mass by size exclusion chromatography (SEC), eluent 0.5 wt% LiBr in NMP, and calibration by narrowly distributed poly(methyl methacrylate) standards^cDispersity index^dMonomer concentration 16 wt%^eYield is given in lieu of conversion^fData taken from ref. [69]^gData taken from ref. [101]^hMonomer concentration of 20 wt%ⁱMonomer concentration of 25 wt%^jMonomer concentration of 34 wt%

were prepared by first dissolving the polymer with the target concentration in water as well as in the pure co-solvent and subsequently combining the desired proportions of the polymer solutions in water and the co-solvent, respectively.

Fourier transform infrared spectroscopy (FTIR) spectra of powders were recorded using a Nicolet Avatar 370 FT-IR spectrometer equipped with an ATR Smart Performer element and AMTIR crystal.

Elemental analysis (EA) used a FlashEA 1112 CHNS/O Automatic Elemental Analyzer with a MAa206R autosampler (Thermo Scientific).

Thermogravimetric analysis (TGA) was conducted using a Mettler Toledo TGA/SDTA851e apparatus, under N₂ atmosphere (20 mL min⁻¹) in the temperature range from 25 to 900 °C, with a heating rate of 10 K min⁻¹. Differential scanning calorimetry (DSC) analyses were performed with

a Mettler Toledo DSC822e device, under N_2 atmosphere (20 mL min^{-1}) at temperatures ranging from 0 to $230 \text{ }^\circ\text{C}$ in four subsequent heating–cooling cycles. Heating and cooling rates were 10 K min^{-1} during the first and second cycles and 30 K min^{-1} during the third and fourth cycles. Glass transition temperatures were derived from the second heating curve, at the mid-point (half height) of the transition step.

Results and discussion

Polymer synthesis and characterization

The polymer pNVIBAm can be obtained by conventional radical polymerization of its monomer NVIBAm in solution [56, 63, 83] using azo initiators. Still, the originally reported synthesis of the monomer is cumbersome, implying a pyrolysis step [83]. Therefore, pNVIBAm was prepared alternatively by post-polymerization modification via a complex three-step sequence. Polymerizing the commercially available monomers *N*-vinyl formamide and *N*-vinylacetamide first, the amide moieties of the precursor polymer obtained were subsequently hydrolyzed to produce poly(vinylamine) as intermediate, which finally was converted to pNVIBAm by reforming the amide moieties with isobutyric acid [84, 85]. As inherently, this pathway may suffer from incomplete functionalization or side reactions, the exact structure of such pNVIBAm samples can deviate from the ideal structure, and therefore, the accuracy of the determined phase transition temperatures (of about $41 \text{ }^\circ\text{C}$) can be questioned. The situation improved considerably with the much simpler synthesis procedure for monomer NVIBAm reported recently [81], which was adapted by us (see the Supplementary Information). In analogy to early reports [83], we employed benzene as solvent for the polymerizations that is highly inert against radical attack. As vinylamides belong to the group of “less activated monomers” [86], the propagating radicals of their polymers are less stabilized and thus, much more reactive and prone to side reactions (such as chain transfer to the solvent), which we wanted to minimize. Also, we tested the use of two different azo initiators, namely AIBN and MAIB (Fig. 2), which feature a very similar thermal decomposition profile, but showed remarkably different initiation efficiencies for the polymerization of monomers that are difficult to polymerize [87–89]. Moreover, NVIBAm was polymerized in the presence of chain transfer agent *S*-cyanomethyl *N*-methyl-*N*-phenyl-carbamodithioate (CTA-X), which was reported to efficiently control the radical addition fragmentation chain transfer polymerization (RAFT) of “less activated monomers” such as vinylamides [90], to prepare a pNVIBAm sample of low molar mass. Table 1 summarizes key reaction conditions and parameters of the polymers produced.

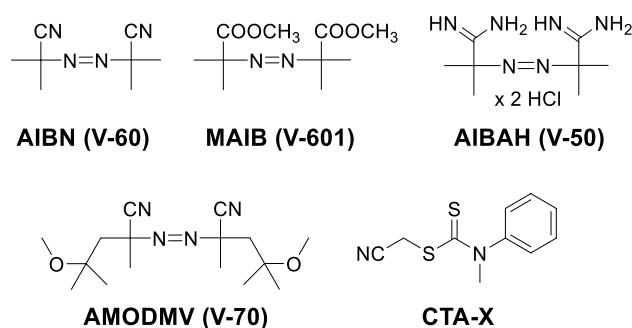


Fig. 2 Chemical structure of the azo initiators employed in the polymerization of NVIBAm and NIPMAM, and of the chain transfer agent *S*-cyanomethyl *N*-methyl-*N*-phenylcarbamodithioate (CTA-X)

The data compiled in Table 1 are not surprising. The conventional radical polymerization of NVIBAm is rather fast (but considerably slowed down in the case of the RAFT process; see entry 6), gives reasonable yields, and delivers a certain spread of polymer molar masses in the range of 30 to 120 kg mol^{-1} for the number average (M_n). The rather moderate values of the dispersity (D) for a conventional free radical polymerization up to high conversions are explained by the purification of the polymers by dialysis and/or precipitation, thus cutting off the low molar mass fraction. The use of either AIBN or MAIB as an initiator did not result in significant differences.

As only very few molecular analytical data on pNVIBAm have been published [58], exemplary ^1H and ^{13}C NMR spectra are shown in Fig. 3 (see also Supplementary Information Figs. S4–S8). Presumably, the complex form of the broad signal between 1.4 and 1.9 ppm (Fig. 3a, signal a), which is characteristic for the methylene protons on the backbone, is due to the polymer’s tacticity. Analogously, tacticity effects may also explain the width and complexity of the corresponding signal between 37 and 42 ppm in the ^{13}C spectrum, which required extended sampling to be distinguishable from the background noise (Fig. 3b; see also Supplementary Information Fig. S6). Though the effects are less pronounced in the spectra, the same consideration applies to the complex form of the signal between 2.3 and 2.6 ppm in the ^1H spectrum (Fig. 3a, signal d) that is characteristic for the methine proton of the isobutyramide moiety of the side chain. Also in this case, the corresponding signal group between 35 and 35.5 ppm in the ^{13}C spectrum consists of at least two only partially resolved signals (see Supplementary Information Fig. S5). Furthermore, the broadened signal b around 3.8 ppm of the backbone methine groups and signal e around 1.1 ppm of the methyl groups being part of the isobutyramide moiety in the side chain in the ^1H spectrum have complex signal counterparts in the ^{13}C spectrum (see Supplementary Information Figs. S4 and S7). Moreover, signal c around 180 ppm of the carbonyl group shows a complex fine

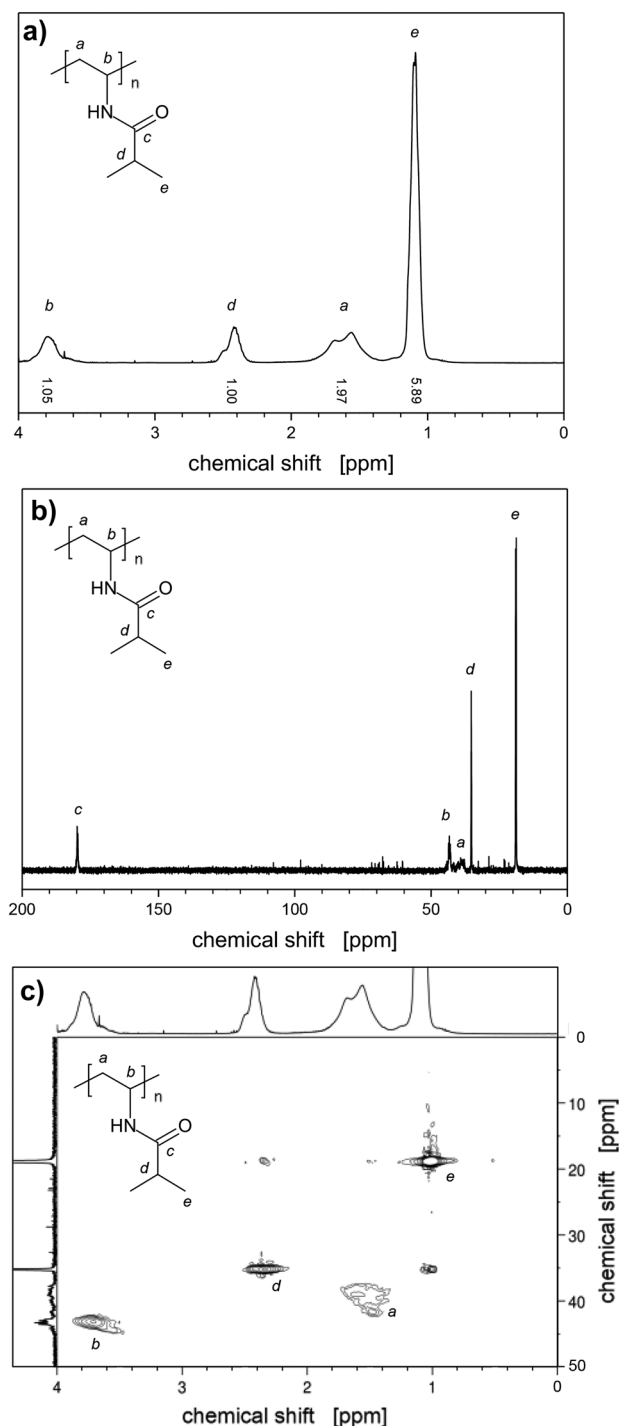


Fig. 3 Exemplary NMR spectra of pNVIBAm in D₂O: **a**) ¹H spectrum (400 MHz); **b**) ¹³C spectrum (151 MHz); **c**) ¹H–¹³C heteronuclear single-quantum correlation (HSQC) spectra

structure at a closer look (see Supplementary Information Fig. S8). All these observations support the view that stereochemical effects in the backbone are responsible for the complex spectral details. However, to our knowledge, literature reports elucidating the influence of the tacticity on the

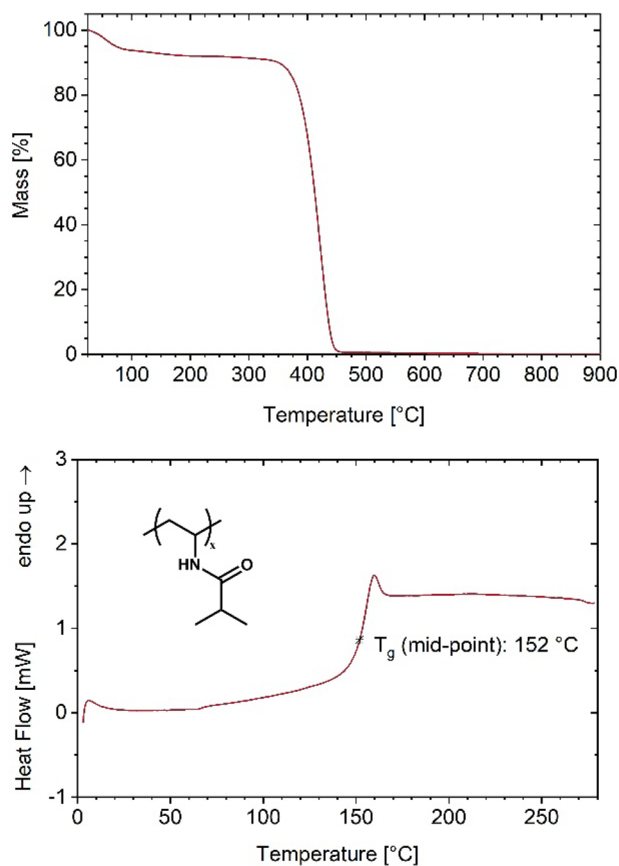


Fig. 4 TGA (top) and DSC (bottom, second heating cycle) thermograms of homopolymer pNVIBAm₃₇₇ (heating rates 10 K min⁻¹)

form of the ¹H spectra of pNVIBAm are missing yet. Hence, we could not attribute the stereochemistry of the pNVIBAm samples from the simple analysis of the ¹H NMR spectra. Nevertheless, their very similar forms indicate that all the samples have virtually the same stereochemistry. Thus, any possible differences of the phase transition temperature in aqueous media (vide infra) cannot be explained by differing tacticities of the polymer samples.

Thermal analysis by thermogravimetry and DSC revealed that pNVIBAm becomes unstable above 300 °C (Fig. 4), but there is no indication for a catastrophic decomposition at 200 °C (which is difficult to rationalize, considering the polymer's chemical structure lacking thermally labile groups) as was reported before [91]. The gradual, limited mass loss occurring largely in the range up to 120 °C results from the evaporation of water bound due to the polymer's marked hygroscopy. After removing the water during the first heating cycle, DSC shows a stable glass transition at about 152 °C (Figs. 4b and S12), considerably higher than the value of 133 °C reported in the aforementioned study [91]. Interestingly, the value of 152 °C is higher than that of its “structural isomer” atactic pNIPAm of about 130–140 °C

[46, 92–94], suggesting that the interaction between the polymer chains is somewhat stronger in the case of atactic pNVIBAm.

In contrast to NVIBAm, the methacrylamide NIPMAM belongs to the group of “more activated monomers,” and thus, its radical polymerization is expected to be less sensitive to side reactions than the one of the vinylamide NVIBAm. Still, a survey of the (surprisingly limited) previous reports on the conventional radical polymerization of NIPMAM reveals that mostly, polymers with low molar masses, i.e., well below 50×10^3 Da, have been produced [28, 64, 65, 74, 95–100]. This includes our previous reported syntheses of pNIPMAM by conventional radical polymerization in THF [69, 101]. In line with these observations, the molar mass of statistical copolymers of NIPAM and NIPMAM drastically decreases with increasing NIPMAM content in the polymerization system [66]. Higher molar masses were typically reported only for aqueous polymerizations using peroxide initiators [70, 102]. Such conditions, however, favor chain transfer to the polymer and cross-linking side reactions via the methine moiety in the side chain that is particularly vulnerable to radical attack, as exploited in the synthesis of microgels from NIPAM and NIPMAM [103].

In order to obtain a set of pNIPMAM samples covering also the high molar mass range ($> 10^5$ Da), we varied largely the polymerization conditions with respect to the reaction solvent, monomer concentration, and concentration and type of initiator (cf. Figure 2). The reaction temperatures were chosen such that the half-life times of the respective initiators used were in the order of 10 h (Table 2).

Compared to the polymerization of NVIBAm, the polymerization of NIPMAM was much more sluggish. Also, we noted that the outcome of the polymerizations with respect to conversion/yield and molar mass obtained was difficult to reproduce, and results varied substantially, in particular when aiming at high molar masses by engaging only minute amounts of initiator. Still, there is a clear trend that high molar masses require rather high monomer concentrations (≥ 30 wt%) and low initiator concentrations (≤ 0.1 mol% relative to monomer), rendering these reactions highly sensitive to the presence of trace impurities. Also, it appears that the use of solvent benzene or trifluoroethanol (TFE), which are highly inert to the attack by carbon-centered radicals, favors high molar masses. None of these specific findings seems surprising, whereas the general troublesomeness to obtain elevated molar masses for pNIPMAM is. Possibly, this behavior is due to a slow propagation rate, rendering the homopolymerization vulnerable against side reactions. A clarification of this hypothesis by detailed kinetic studies seems interesting, but was beyond the scope of our study. In any case, we produced a large set of pNIPMAM samples in this way with molar masses (M_n) between 7 and 150×10^3 Da.

The ^1H NMR spectra of the various pNIPMAM samples synthesized looked very similar (Fig. 5a), corresponding closely to the ones in the literature of samples also prepared by conventional radical polymerization in solution [66, 79]. Unfortunately, the complex signal group of the protons of the

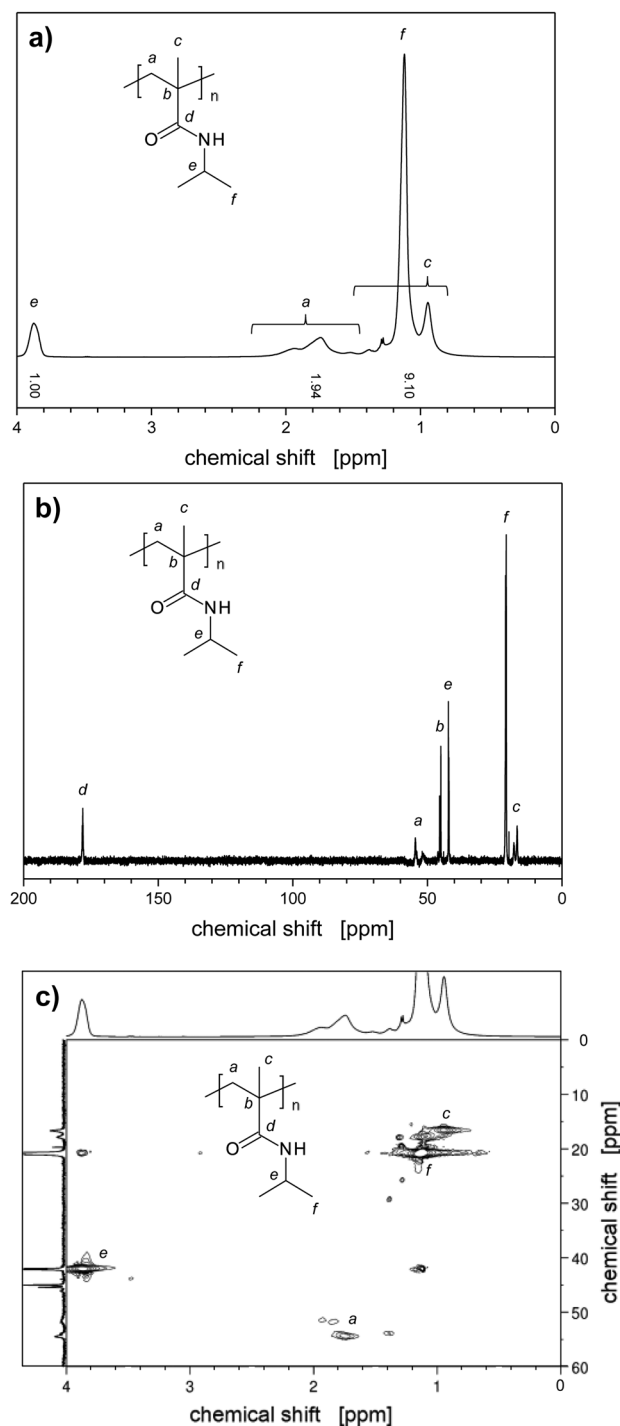


Fig. 5 Exemplary NMR spectra of pNIPMAM in D_2O : **a)** ^1H spectrum (500 MHz); **b)** ^{13}C spectrum (126 MHz); **c)** ^1H - ^{13}C heteronuclear single-quantum correlation (HSQC) spectra

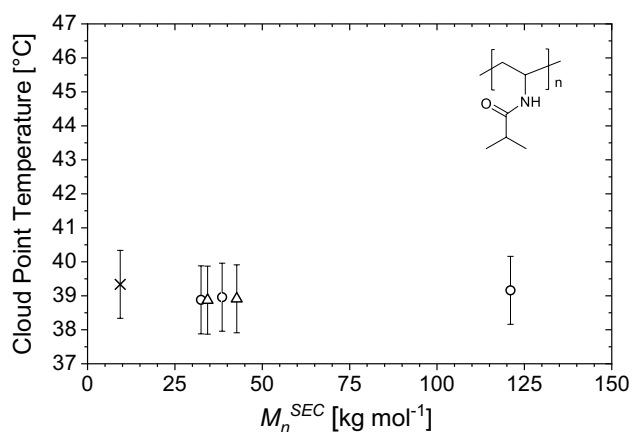


Fig. 7 Effect of molar mass and end groups on cloud point of pNVIBAm (10 g L^{-1} in water, $\lambda=500 \text{ nm}$), using the initiators MAIB (white circle) and AIBN (white triangle), or, additionally, the chain transfer agent CTA-X (X)

[109], or poly(*N,N*-bis(2-methoxyethyl)acrylamide) [110], for which the minimum of the cloud point continuously shifts to lower concentration with increasing molar mass, thus approaching finally the value of 0 at infinitely high molar masses.

Moreover, for a given concentration, the cloud point temperature (T_{CP}) seems not to vary significantly within the accuracy of the measurements for different molar masses when a value of 20 kg mol^{-1} is exceeded (Fig. 7). All these findings are in agreement with an LCST behavior of type II, corroborating a previous report on pNVIBAm-based hydrogels [56]. Also, no significant difference was found for polymer samples which were prepared using the different initiators (AIBN or MAIB or RAFT agent), thus resulting in end groups of somewhat differing polarities/hydrophilicities.

The thermoresponsive behavior of dilute and semi-dilute aqueous solutions of pNIPMAm is exemplified in Figs. 8, 9, and 10. It shows many similarities to the behavior of pNVIBAm. Nevertheless, it should be kept in mind that the solubility–insolubility phase transition of pNIPMAm in aqueous solution features some particularities compared to the classical case of, e.g., pNIPAm [76]. The transition temperatures of pNIPMAm determined by different methods may deviate significantly, e.g., when studied by turbidimetry or by calorimetry, where T_{CP} is systematically lower than calorimetric transition temperature (T_{DSC}) [69]. Also, the clouding transition is prone to a more marked hysteresis between the heating (resulting in clouding) and cooling (resulting in clearing) runs [69, 76], but this seems also true for pNVIBAm. The hysteresis behavior is illustrated for the high molar mass samples pNVIBAm₁₀₆₉ and pNIPMAm₉₅₆ in Fig. 8. Further, pNIPMAm tends to sediment/precipitate rapidly once heated above the cloud point (*cf.* the apparent increase in transmittance upon continuous heating in Fig. 9 that results

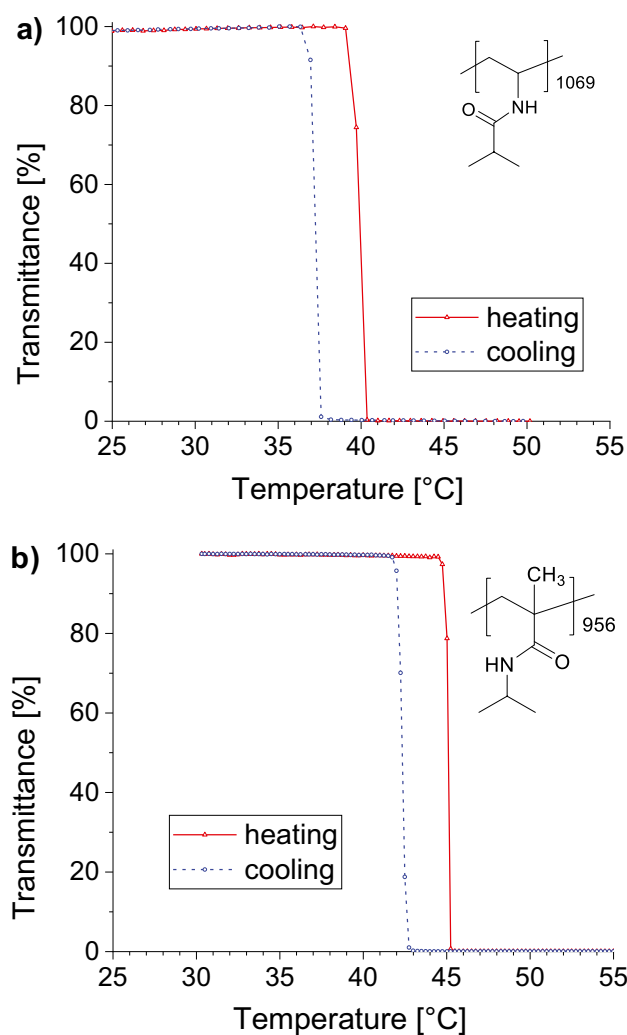


Fig. 8 Hysteresis of the clouding and clearing behavior of aqueous solutions (10 g L^{-1}): **a**) pNVIBAm₁₀₆₉; **b**) pNIPMAm₉₅₆ in heating (continuous red line) and cooling (broken blue line) cycles; $\lambda=500 \text{ nm}$, heating and cooling rates 0.5 K min^{-1}

from colloid sedimentation), whereas colloids of collapsed pNVIBAm above the cloud point tend to stay dispersed for much longer periods, forming so-called mesoglobules, as they are well-established in the case of pNIPAm [4].

As the majority of the reports on the thermal behavior of pNIPMAm have focused on turbidimetric studies of the clouding upon heating, we also confined our screening of the thermal behavior of pNIPMAm solutions to the clouding transition by turbidimetry (Figs. 9 and 10). Figure 9a displays typical transmittance curves in dependence on the temperature for the high molar mass sample pNIPMAm₉₅₆. The polymers feature a sharp clouding transition upon heating at about 44 °C , which exhibits a continuous small but significant decrease with increasing concentration of up to at least 50 g L^{-1} even for the highest molar masses studied (Fig. 9b, see also Supplementary Information Figs. S14 and S16).

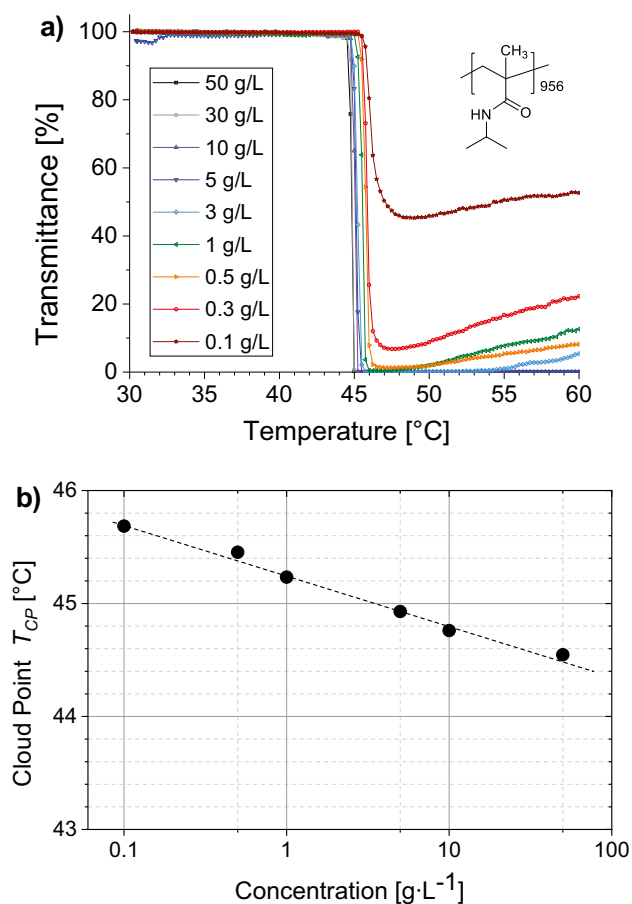


Fig. 9 Behavior of pNIPMAm₉₅₆ in pure aqueous solution: **a)** Temperature and concentration dependence of the transmittance ($\lambda=500$ nm, heating rate 0.5 K min^{-1}); **b)** Concentration dependence of the cloud point. Precision ± 0.2 °C, accuracy ± 1 °C. The dashed line is meant as a guide to the eye

Furthermore, for a given concentration, the cloud point does not vary significantly within the accuracy of the measurements for different molar masses, at the least when a value of 20 kg mol^{-1} is exceeded (Fig. 10), and takes a value of about 44.5 °C, with the notable exception of the samples prepared with the initiator AMODMV/V70. The latter group shows also a cloud point independent of the molar mass, but at about 41 °C, i.e., $3\text{--}4$ °C lower than for the other pNIPMAm samples.

One possible reason for this difference could be that the lower polymerization temperature of these samples and/or that the choice of ethanol as reaction medium changes the stereochemistry of pNIPMAm and induces, for instance, a higher degree of isotactic triads [95]. However, such an explanation is not compatible with the close similarity of all NMR spectra of the various pNIPMAm made (see above). It would be also difficult to reconcile with the reports that notable differences in the stereochemistry for poly(meth)acrylamides such as pNIPAm or poly(*N*-methyl

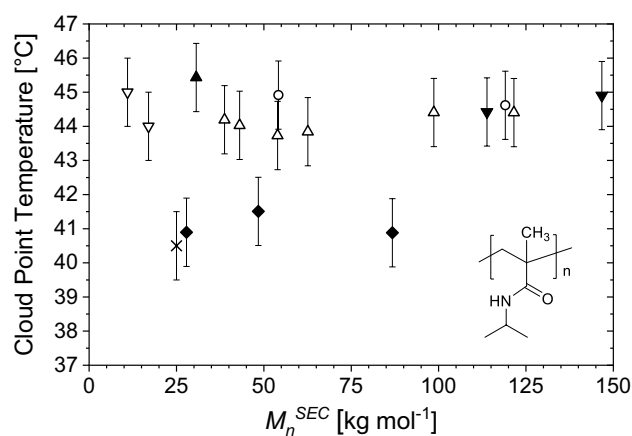


Fig. 10 Effect of molar mass and end groups on the cloud point of pNIPMAm (10 g L^{-1} in water, $\lambda=500$ nm), using the initiators MAIB in benzene (white circle), AIBN in benzene (white triangle), AIBN in THF (white upside-down triangle), AIBN in TFE (filled triangle), AIBA in TFE (filled upside-down triangle), and AMODMV in ethanol (filled diamond) or using a chain transfer agent bearing a hydrophobic dye (X, data taken from ref. [68])

methacrylamide) produced by radical polymerization are only obtained, if conducted at considerably lower temperatures than employed in our study and in highly fluorinated solvents [105, 111], or when complexing agents are specifically added [95, 104]. This is not the case here. Therefore, in analogy to previous reports on the lowering of the cloud point of pNIPMAm when attaching hydrophobic end groups of intermediate size [68], we putatively attribute the relatively low cloud points to the end groups derived from the initiator fragments. These are considerably more hydrophobic in the case of initiator AMODMV than in the case of initiators AIBN, MAIB, and AIBA (*cf.* Figure 2). Anyhow, as observed for pNVIBAm, all findings support the view that also pNIPMAm exhibits LCST behavior of type II.

Co-nonsolvency behavior in mixtures of water and organic solvents

The co-nonsolvency of pNIPAM in mixed aqueous solutions is well established, with the focus on the solvent system water–methanol [50, 112–120]. Occasionally, co-nonsolvency behavior was also reported for other organic co-solvents. Presumably, the broadest study of co-nonsolvency in various co-solvents is that by Costa and Freitas [121], where co-nonsolvency of pNIPAM with the co-solvents methanol, ethanol, isopropyl alcohol, *n*-propanol, acetone, DMSO, and DMF was compared. Further, acetonitrile, glycerol, oligoethyleneglycols, THF, and 1,4-dioxane were reported to show co-nonsolvency for pNIPAM [22, 122, 123]. Still, the reasons for the occurrence of co-nonsolvency are not clear yet, including a debate whether or not co-nonsolvency is a generic

phenomenon, which does not depend on the specific interactions between the components of the system [124, 125]. Importantly, two contrasting patterns of co-nonsolvency have been reported for pNIPAm [121]. In the first pattern, the LCST transition passes through a minimum value with an increasing fraction of co-solvent. This is the case for the co-solvents methanol, acetone, THF, and dioxane. In the second pattern, the LCST transition decreases continuously until it falls below the melting point of the solvent mixtures, but does not recover for high fractions of co-solvent. Instead, the increasing fraction of co-solvent causes the UCST transition to decline steeply, until solubility is regained for a given temperature [126]. The latter scenario seems to be the more frequent one [121], applying to most other alcohols studied as well as to DMF and DMSO as co-solvent. However, many studies that have dealt with the swelling of gels in mixed aqueous media could not distinguish these two scenarios, e.g., when just following the reentrant swelling effect at a constant temperature as frequently done. In view of these observations, we screened the possible co-nonsolvency behavior in mixed aqueous solutions for a variety of co-solvents up to a molar fraction of 0.3 for pNIPAm and pNVIBAm and compared their behaviors to that of their analogue pNIPAm using data from the literature (Figs. 11, 12, and 13), within the temperature window of 14 to 60 °C accessible by our experimental set-up.

Figure 11 illustrates the effect of lower alcohols as co-solvents, namely of methanol, ethanol, *iso*-propanol, and *n*-propanol, on the cloud points of pNVIBAm (Fig. 11a) and pNIPMAM (Fig. 11b) in comparison to pNIPAm. All three polymers show qualitatively a similar behavior in the particular water–alcohol mixtures, and for a specific concentration and mixture, the transition temperatures always decrease in the order pNIPMAM > pNVIBAm > pNIPAm. Throughout, the extent of the co-nonsolvency effect, i.e., the magnitude of the decrease of T_{CP} , increases with the decrease of the alcohol's polarity. Methanol produces the mildest effects, while *n*-propanol provokes the strongest ones. In the case of methanol, a minimum for T_{CP} is attained at about 30 mol% of co-solvent in water, beyond which the coexistence line increases rather steeply and the solubility window re-opens (scenario 1). Looking in more detail, the reduction of T_{CP} is considerably more prominent for pNIPAm than for pNVIBAm and pNIPMAM, which show comparable strengths of the effect. We also note that the amount of methanol in the mixtures, at which the cloud point is minimum, decreases from about 35 mol% for pNIPAm via about 31 mol% for pNVIBAm to about 29 mol% for pNIPMAM. For ethanol, *iso*-propanol, and *n*-propanol, no increase of T_{CP} could be observed at intermediate alcohol contents in the concentration and temperature window studied, suggesting a behavior according to pattern 2 (change from LCST to UCST transition). In any case, all three polymers

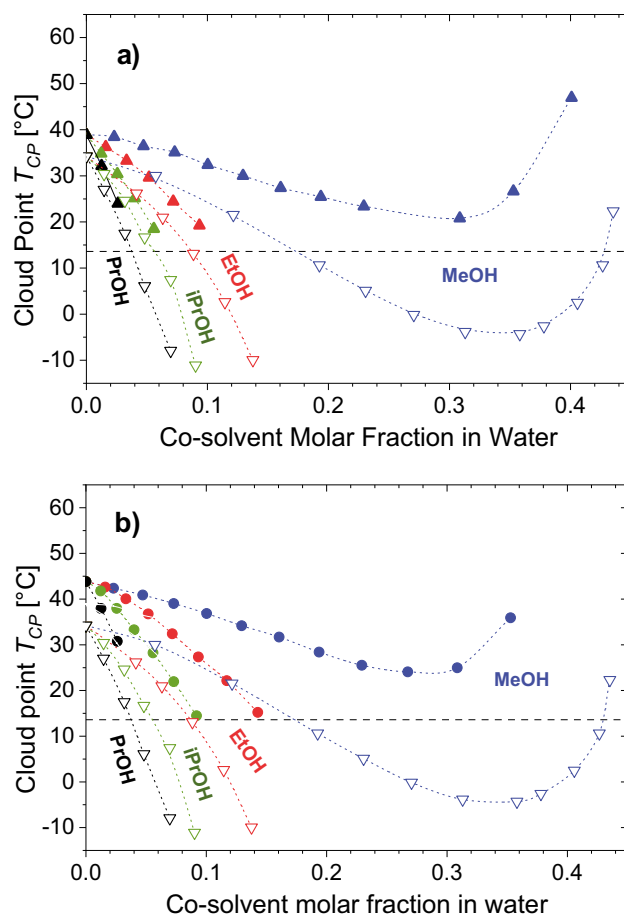


Fig. 11 Co-nonsolvency in mixtures of water and lower alcohols (methanol (MeOH, blue), ethanol (EtOH, red), *iso*-propanol (i-PrOH, green), and *n*-propanol (PrOH, black): **a**) of pNVIBAm (full symbols: blue, red, green, and black triangles); **b**) of pNIPMAM (full symbols: blue, red, green, and black circles), followed by the cloud point ($\lambda=500$ nm, heating rate 0.5 K min^{-1}). The dashed curves are meant as a guide to the eye. For comparison, the corresponding solutions of pNIPAm are shown (open symbols: blue, red, green, and black upside-down triangles) with data from reference [121]. The horizontal broken black line indicates the lower temperature limit of the experimental set-up used

become soluble at room temperature in alcohol-rich aqueous solutions.

Figure 12 illustrates the effect of aprotic polar co-solvents, namely DMF, DMSO, and acetone, on the cloud points of pNIPMAM and pNVIBAm. Acetone imparts on both pNIPMAM and pNVIBAm a similar behavior as methanol does, following co-nonsolvency pattern 1, albeit with a more pronounced effect on T_{CP} (shift to lower temperatures). For pNVIBAm, DMSO and DMF have a similar impact on the transition temperatures as what was reported for pNIPAm (Fig. 12a). DMSO shows little impact when present in low fractions but causes T_{CP} to drop more strongly as the fraction of co-solvent increases. The effect of DMF looks similar at a first view. However, low fractions of the co-solvent induce

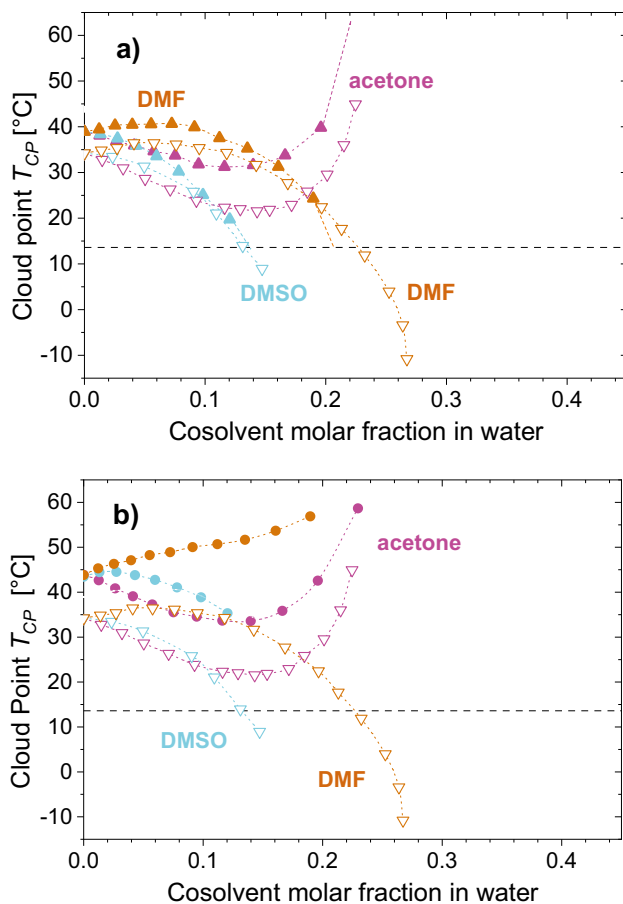


Fig. 12 Co-nonsolvency in mixtures of water and dipolar aprotic solvents (DMSO (cyan), DMF (brown), and acetone (magenta)): **a)** of pNVIBAM (full symbols: cyan, brown, and magenta triangles); **b)** of pNIPMAM (full symbols: cyan, brown, and magenta circles), followed by the cloud point ($\lambda=500$ nm, heating rate 0.5 K min^{-1}). The dashed curves are meant as a guide to the eye. For comparison, the corresponding solutions of pNIPAM are shown (open symbols: cyan, brown, and magenta upside-down triangles) with data from reference [121]. The horizontal broken black line indicates the lower temperature limit of the experimental set-up used

a slight increase of T_{CP} , up to a molar fraction of about 0.07, corroborating previous observations [22, 121], above which T_{CP} starts to fall continuously. The behavior of pNIPMAM in aqueous mixtures with DMSO and DMF, however, shows particularities. Most prominently, the addition of DMF makes T_{CP} to rise continuously with no sign of co-nonsolvency behavior. The addition of DMSO results in a complicated behavior. Initially, it results in a slight increase of the transition temperature of pNIPMAM up to a molar fraction of ca. 0.025, only beyond which T_{CP} decreases in the typical co-nonsolvency fashion. Interestingly, while Costa and Freitas [121] did not report a similar effect, Yamauchi and Maeda [127] observed an analogous behavior for pNIPAM with a small maximum of T_{CP} at a comparably small molar fraction of DMSO before inducing co-nonsolvency at higher fractions.

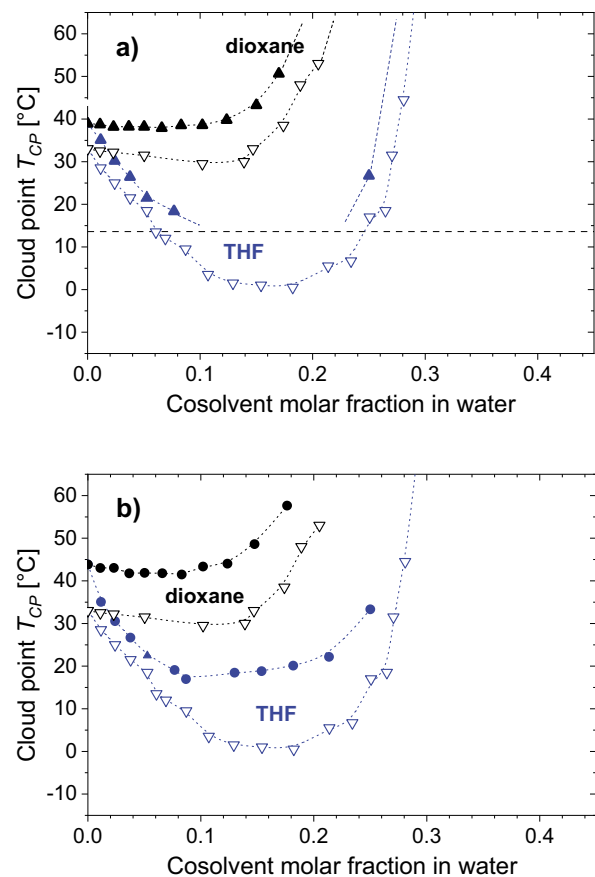


Fig. 13 Co-nonsolvency in mixtures of water and dipolar aprotic solvents (THF (blue) and dioxane (black)): **a)** of pNVIBAM (full symbols: black and blue triangles); **b)** of pNIPMAM (full symbols: black and blue circles), followed by the cloud point ($\lambda=500$ nm, heating rate 0.5 K min^{-1}). The dashed curves are meant as a guide to the eye. For reference, the corresponding solutions of pNIPAM are shown (open symbols: black and blue upside-down triangles) using data from reference [122]. The horizontal broken black line indicates the lower temperature limit of the experimental set-up used

The effect of adding the cyclic ethers THF and dioxane on the cloud points of pNIPMAM and pNVIBAM is illustrated in Fig. 13. For both pNIPAM and pNVIBAM, already small THF contents in water cause a very sharp drop of the transition temperature (Fig. 13a). For pNIPMAM, a first small, and then increasingly marked increase of T_{CP} is observed when the molar fraction of THF exceeds 0.1 (Fig. 13b). The analogous behavior was observed for pNVIBAM, though the lowest transition temperatures were outside of the measuring range of our experimental setup.

Finally, co-nonsolvency of pNIPMAM and pNVIBAM in water–dioxane mixtures was evaluated, for which only weak co-nonsolvency behavior has been reported for pNIPAM [122, 128]. For both pNVIBAM and pNIPMAM, an even weaker, nearly plateau-like effect of lowering T_{CP} is observed in mixtures with dioxane molar fractions below 0.1

(Fig. 13). The effect is small for pNIPMAm (for which T_{CP} is reduced by about 2 °C at maximum at a molar fraction of 0.08, Fig. 13b) and even marginal for pNVIBAm (for which T_{CP} is reduced by 0.7 °C at maximum for a molar fraction of 0.05, Fig. 13a), while T_{CP} increases steeply for both polymers when the molar fraction of dioxane is further increased. This behavior may be interesting from a practical point of view when amphiphilic block copolymers combining thermoresponsive blocks of pNIPAm, pNVIBAm, or pNIPMAm and a hydrophobic block such as polystyrene are to be dispersed in water to form small micellar entities or nanoparticles, by continuously diluting a solution of the block copolymer in a nonselective, water-miscible solvent with water [129, 130]. With dioxane being a good solvent for many polymers, the homogeneous solutions of such block copolymers in dioxane can be continuously diluted at ambient temperature to make the hydrophobic block micro-phase separate without the interfering intermediate precipitation and aggregation of both the hydrophobic and the thermoresponsive hydrophilic blocks, as encountered for most fully water-miscible organic solvents.

Overall, the co-nonsolvency behaviors of pNIPMAm and pNVIBAm appear qualitatively comparable to that of pNIPAm, but are quantitatively less pronounced, with transition temperatures consistently following the trend of pNIPAm < pNVIBAm < pNIPMAm. Nevertheless, some differences were identified. The most remarkable one seems that DMF does not cause co-nonsolvency for pNIPMAm (Fig. 12b), contrary to the marked co-nonsolvency effect encountered for both pNIPAm and pNVIBAm (Fig. 12a). Whereas the rather close similarities of the overall co-nonsolvency behaviors of the “isomeric” polymers pNIPAm and pNVIBAm are not self-evident but seem intuitively comprehensible, this is less obvious for the case of pNIPMAm. As already the interaction with water differs notably, resulting in a considerably higher LCST for pNIPMAm despite a formally lower hydrophilic-lipophilic balance of the repeat unit (see “Introduction”), more differences in the co-nonsolvency behavior than the few observed might have been expected. As, however, our understanding of the co-nonsolvency phenomenon is quite limited (and disputed) yet, a convincing explanation has to be awaited for.

Conclusions

Both analogues of poly(*N*-isopropyl acrylamide) (pNIPAm), namely poly(*N*-vinyl isobutyramide) (pNVIBAm) and poly(*N*-isopropyl methacrylamide) (pNIPMAm), feature an upper miscibility gap in aqueous solution, for which the phase transition temperatures hardly evolve above molar

masses of 20 kg mol⁻¹. As, furthermore, the phase transition temperatures decrease still gradually with increasing polymer concentration up to a concentration of at least 50 g L⁻¹ even for high molar masses, both polymers seem to feature the unusual LCST type II behavior that is characteristic for pNIPAm [26]. Overall, differences in the properties compared to pNIPAm seem somewhat more pronounced for pNIPMAm than for pNVIBAm. For a given polymer concentration, phase transition temperatures increase in the order pNIPAm < pNVIBAm < pNIPMAm, which cannot be intuitively rationalized simply by the relative hydrophilicities of the repeat units chemical structures. As known for pNIPAm, both pNVIBAm and pNIPMAm exhibit marked co-nonsolvency behavior with a large group of water-miscible organic solvents, including lower alcohols, as well as aprotic solvents of different polarities such as dimethylsulfoxide (DMSO), acetone, and tetrahydrofuran (THF). Both pNVIBAm and pNIPMAm show also co-nonsolvency in mixtures of water and dioxane, but the effects are marginal, even weaker than known for pNIPAm. Throughout, the co-nonsolvency behavior becomes less pronounced in the order pNIPAm > pNVIBAm > pNIPMAm. Exceptionally, pNIPMAm does not feature co-nonsolvency in mixtures of water and *N,N*-dimethylformamide (DMF). In contrast, pNVIBAm shows weak co-solvency at low, but marked co-nonsolvency at intermediate fractions of DMF in the mixtures, as reported for pNIPAm. In mixtures containing DMSO, co-nonsolvency behavior was observed for pNVIBAm for all fractions of the co-solvent, while pNIPMAm shows weak co-solvency at low, but notable co-nonsolvency at intermediate fractions of DMSO. In the light of the current theories about the origin of co-nonsolvency [48, 50, 131, 132], these observations are difficult to explain and might trigger further investigations and atomistic simulations. In any case, the many similarities of their thermoresponsive behaviors to the one of pNIPAm, together with the difference in the transition temperatures, render pNVIBAm and pNIPMAm interesting complements to pNIPAm as building blocks for smart polymers.

Supplementary Information The online version contains supplementary material available at <https://doi.org/10.1007/s00396-023-05083-4>.

Acknowledgements The authors acknowledge the support for SEC analysis by S. Prenzel and H. Schlaad, the support for thermal analysis by A. Taubert, and the support for NMR spectroscopy by A. Krtitschka and H. Möller (all University of Potsdam).

Funding Open Access funding enabled and organized by Projekt DEAL. This study received financial support from the Deutsche Forschungsgemeinschaft DFG (grants LA 611/16–1, MU 1487/29–1, and PA 771/20–1).

Declarations

Conflict of interest The authors declare no competing interests.

Open Access This article is licensed under a Creative Commons Attribution 4.0 International License, which permits use, sharing, adaptation, distribution and reproduction in any medium or format, as long as you give appropriate credit to the original author(s) and the source, provide a link to the Creative Commons licence, and indicate if changes were made. The images or other third party material in this article are included in the article's Creative Commons licence, unless indicated otherwise in a credit line to the material. If material is not included in the article's Creative Commons licence and your intended use is not permitted by statutory regulation or exceeds the permitted use, you will need to obtain permission directly from the copyright holder. To view a copy of this licence, visit <http://creativecommons.org/licenses/by/4.0/>.

References

- Aseyev V, Tenhu H, Winnik F (2006) Temperature dependence of the colloidal stability of neutral amphiphilic polymers in water. *Adv Polym Sci* 196:1–85
- Tavagnacco L, Zaccarelli E, Chiessi E (2022) Modeling solution behavior of poly(N-isopropylacrylamide): a comparison between water models. *J Phys Chem B* 126:3778–3788. <https://doi.org/10.1021/acs.jpcc.2c00637>
- Niebuur B-J, Chiappisi L, Zhang X, Jung F, Schulte A, Papadakis CM (2018) Formation and growth of mesoglobules in aqueous poly(N-isopropylacrylamide) solutions revealed with kinetic small-angle neutron scattering and fast pressure jumps. *ACS Macro Lett* 7:1155–1160. <https://doi.org/10.1021/acsmacrolett.8b00605>
- Aseyev V, Tenhu H, Winnik F (2011) Non-ionic thermoresponsive polymers in water. *Adv Polym Sci* 242:29–89. https://doi.org/10.1007/12_2010_57
- Roy D, Brooks WLA, Sumerlin BS (2013) New directions in thermoresponsive polymers. *Chem Soc Rev* 42:7214–7243. <https://doi.org/10.1039/c3cs35499g>
- Zhao C, Ma Z, Zhu XX (2019) Rational design of thermoresponsive polymers in aqueous solutions: a thermodynamics map. *Prog Polym Sci* 90:269–291. <https://doi.org/10.1016/j.progpolymsci.2019.01.001>
- Hannappel Y, Wiehemeier L, Dirksen M, Kottke T, Hellweg T (2021) Smart microgels from unconventional acrylamides. *Macromol Chem Phys* 222(2100067):2100061–2100013. <https://doi.org/10.1002/macp.202100067>
- Priest JH, Murray SL, Nelson RJ, Hoffman AS (1987) Lower critical solution temperatures of aqueous copolymers of N-isopropylacrylamide and other N-substituted acrylamides. *ACS Symp Ser* 350:255–264. <https://doi.org/10.1021/bk-1987-0350.ch018>
- Laschewsky A, Rekaï ED, Wischerhoff E (2001) Tailoring of stimuli-responsive water-soluble acrylamide and methacrylamide polymers. *Macromol Chem Phys* 202:276–286. [https://doi.org/10.1002/1521-3935\(20010101\)202:2%3c276::aid-macp276%3e3.0.co;2-1](https://doi.org/10.1002/1521-3935(20010101)202:2%3c276::aid-macp276%3e3.0.co;2-1)
- Lutz J-F, Weichenhan K, Akdemir Ö, Hoth A (2007) About the phase transitions in aqueous solutions of thermoresponsive copolymers and hydrogels based on 2-(2-methoxyethoxy)ethyl methacrylate and oligo(ethylene glycol) methacrylate. *Macromolecules* 40:2503–2508. <https://doi.org/10.1021/ma062925q>
- ten Brummelhuis N, Schlaad H (2011) Stimuli-responsive star polymers through thiol–yne core functionalization/crosslinking of block copolymer micelles. *Polym Chem* 2:1180–1184. <https://doi.org/10.1039/c1py00002k>
- Weiss J, Li A, Wischerhoff E, Laschewsky A (2012) Water-soluble random and alternating copolymers of styrene monomers with adjustable lower critical solution temperature. *Polym Chem* 3:352–361. <https://doi.org/10.1039/c1py00422k>
- Furyk S, Zhang Y, Ortiz-Acosta D, Cremer PS, Bergbreiter DE (2006) Effects of end group polarity and molecular weight on the lower critical solution temperature of poly(N-isopropylacrylamide). *J Polym Sci, Part A: Polym Chem* 44:1492–1501. <https://doi.org/10.1002/pola.21256>
- Xia Y, Burke NAD, Stöver HDH (2006) End group effect on the thermal response of narrow-disperse poly(N-isopropylacrylamide) prepared by atom transfer radical polymerization. *Macromolecules* 39:2275–2283. <https://doi.org/10.1021/ma0519617>
- Isobe Y, Fujioka D, Habaue S, Okamoto Y (2001) Efficient Lewis acid-catalyzed stereocontrolled radical polymerization of acrylamides. *J Am Chem Soc* 123:7180–7181. <https://doi.org/10.1021/ja015888i>
- Katsumoto Y, Etoh Y, Shimoda N (2010) Phase diagrams of stereocontrolled poly(N, N-diethylacrylamide) in water. *Macromolecules* 43:3120–3121. <https://doi.org/10.1021/ma902673z>
- Nishi K, Hiroi T, Hashimoto K, Fujii K, Han Y-S, Kim T-H, Katsumoto Y, Shibayama M (2013) SANS and DLS study of tacticity effects on hydrophobicity and phase separation of poly(N-isopropylacrylamide). *Macromolecules* 46:6225–6232. <https://doi.org/10.1021/ma401349v>
- Kunugi S, Takano K, Tanaka N, Suwa K, Akashi M (1997) Effects of pressure on the behavior of the thermoresponsive polymer poly(N-vinylisobutyramide) (PNVIBA). *Macromolecules* 30:4499–4501. <https://doi.org/10.1021/ma961770r>
- Kirpach A, Adolf D (2006) High pressure induced coil-globule transitions of smart polymers. *Macromol Symp* 237:7–17. <https://doi.org/10.1002/masy.200650502>
- Niebuur B-J, Claude K-L, Pinzek S, Cariker C, Raftopoulos KN, Pipich V, Appavou M-S, Schulte A, Papadakis CM (2017) Pressure-dependence of poly(N-isopropylacrylamide) mesoglobule formation in aqueous solution. *ACS Macro Lett* 6:1180–1185. <https://doi.org/10.1021/acsmacrolett.7b00563>
- Niebuur B-J, Chiappisi L, Jung F, Zhang X, Schulte A, Papadakis CM (2019) Kinetics of mesoglobule formation and growth in aqueous poly(N-isopropylacrylamide) solutions: pressure jumps at low and at high pressure. *Macromolecules* 52:6416–6427. <https://doi.org/10.1021/acs.macromol.9b00937>
- Panayiotou M, Garret-Flaudy F, Freitag R (2004) Co-nonsolvency effects in the thermoprecipitation of oligomeric polyacrylamides from hydro-organic solutions. *Polymer* 45:3055–3061. <https://doi.org/10.1016/j.polymer.2004.02.046>
- Hofmann C, Schönhoff M (2009) Do additives shift the LCST of poly(N-isopropylacrylamide) by solvent quality changes or by direct interactions? *Colloid Polym Sci* 287:1369–1376. <https://doi.org/10.1007/s00396-009-2103-3>
- Zhang Y, Cremer PS (2010) Chemistry of Hofmeister anions and osmolytes. *Annu Rev Phys Chem* 61:63–83. <https://doi.org/10.1146/annurev.physchem.59.032607.093635>
- Umapathi R, Reddy PM, Rani A, Venkatesu P (2017) Influence of additives on thermoresponsive polymers in aqueous media: a case study of poly(N-isopropylacrylamide). *Phys Chem Chem Phys* 20:9717–9744. <https://doi.org/10.1039/c7cp08172c>
- Afroz F, Nies E, Berghmans H (2000) Phase transitions in the system poly(N-isopropylacrylamide)/water and swelling behaviour of the corresponding networks. *J Mol Struct* 554:55–68. [https://doi.org/10.1016/s0022-2860\(00\)00559-7](https://doi.org/10.1016/s0022-2860(00)00559-7)
- Halperin A, Kröger M, Winnik FM (2015) Poly(N-isopropylacrylamide) phase diagrams: fifty years of research. *Angew Chem Int Ed* 54:15342–15367. <https://doi.org/10.1002/anie.201506663>
- Uchiyama S, Matsumura Y, de Silva AP, Iwai K (2003) Fluorescent molecular thermometers based on polymers showing temperature-induced phase transitions and labeled with

- polarity-responsive benzofurazans. *Anal Chem* 75:5926–5935. <https://doi.org/10.1021/ac0346914>
29. Couturier J-P, Sütterlin M, Laschewsky A, Hettrich C, Wischerhoff E (2015) Responsive inverse opal hydrogels for the sensing of macromolecules. *Angew Chem Int Ed* 54:6641–6644. <https://doi.org/10.1002/anie.201500674>
 30. Couturier J-P, Wischerhoff E, Bernin R, Hettrich C, Koetz J, Sütterlin M, Tiersch B, Laschewsky A (2016) Thermoresponsive polymers and inverse opal hydrogels for the detection of diols. *Langmuir* 32:4333–4345. <https://doi.org/10.1021/acs.langmuir.6b00803>
 31. Enzenberg A, Laschewsky A, Boeffel C, Wischerhoff E (2016) Influence of the near molecular vicinity on the temperature regulated fluorescence response of poly(N-vinylcaprolactam). *Polymers* 8(109):101–127. <https://doi.org/10.3390/polym8040109>
 32. Wei M, Gao Y, Lia X, Serpe MJ (2017) Stimuli-responsive polymers and their applications. *Polym Chem* 8:127–143. <https://doi.org/10.1039/c6py01585a>
 33. Schäfer-Soenen H, Moerkerke R, Berghmans H, Koningsveld R, Dušek K, Šolc K (1997) Zero and off-zero critical concentrations in systems containing polydisperse polymers with very high molar masses. 2. The system water–poly(vinyl methyl ether). *Macromolecules* 30:410–416. <https://doi.org/10.1021/ma960114o>
 34. Han J, Takahashi R, Kuang C, Sato T (2022) Phase Separation behavior of aqueous poly(N-isopropylacrylamide) solutions studied by scattering experiments. *Langmuir* 38:5089–5097. <https://doi.org/10.1021/acs.langmuir.1c01917>
 35. Fujishige S, Kubota K, Ando I (1989) Phase transition of aqueous solutions of poly(N-isopropylacrylamide) and poly(N-isopropylmethacrylamide). *J Phys Chem* 93:3311–3313. <https://doi.org/10.1021/j100345a085>
 36. Inomata H, Goto S, Saito S (1990) Phase transition of N-substituted acrylamide gels. *Macromolecules* 23:4887–4888. <https://doi.org/10.1021/ma00224a023>
 37. Kojima H, Tanaka F (2010) Cooperative hydration induces discontinuous volume phase transition of cross-linked poly(N-isopropylacrylamide) gels in water. *Macromolecules* 43:5103–5113. <https://doi.org/10.1021/ma100588f>
 38. Liu R, Fraylich M, Saunders BR (2009) Thermoresponsive copolymers: from fundamental studies to applications. *Colloid Polym Sci* 287:627–643. <https://doi.org/10.1007/s00396-009-2028-x>
 39. Döring A, Birnbaum W, Kuckling D (2013) Responsive hydrogels – structurally and dimensionally optimized smart frameworks for applications in catalysis, micro-system technology and material science. *Chem Soc Rev* 42:7391–7420. <https://doi.org/10.1039/c3cs60031a>
 40. Laschewsky A, Müller-Buschbaum P, Papadakis CM (2013) Thermo-responsive amphiphilic di- and triblock copolymers based on poly(N-isopropylacrylamide) and poly(methoxy diethylene glycol acrylate): aggregation and hydrogel formation in bulk solution and in thin films. *Prog Colloid Polym Sci* 140:15–34. https://doi.org/10.1007/978-3-319-01683-2_2
 41. Kim Y-J, Matsunaga YT (2017) Thermo-responsive polymers and their application as smart biomaterials. *J Mater Chem B* 5:4307–4321. <https://doi.org/10.1039/c7tb00157f>
 42. Hu L, Zhang Q, Li X, Serpe MJ (2019) Stimuli-responsive polymers for sensing and actuation. *Mater Horiz* 6:1774–1793. <https://doi.org/10.1039/c9mh00490d>
 43. Cook MT, Haddow P, Kirton SB, McAuley WJ (2021) Polymers exhibiting lower critical solution temperatures as a route to thermoreversible gelators for healthcare. *Adv Funct Mater* 31(2008123):2008121–2008125. <https://doi.org/10.1002/adfm.202008123>
 44. Geiger C, Reitenbach J, Henschel C, Kreuzer LP, Widmann T, Wang P, Mangiapia G, Moulin J-F, Papadakis CM, Laschewsky A, Müller-Buschbaum P (2021) Ternary nanoswitches realized with multiresponsive PMMA-b-PNIPMAM films in mixed water/acetone vapor atmospheres. *Adv Eng Mater* 23(2100191):2100191–2100112. <https://doi.org/10.1002/adem.202100191>
 45. Schild HG (1992) Poly(N-isopropylacrylamide): experiment, theory and application. *Prog Polym Sci* 17:163–249
 46. Van Durme K, Van Assche G, Van Mele B (2004) Kinetics of demixing and remixing in poly(N-isopropylacrylamide)/water studied by modulated temperature DSC. *Macromolecules* 37:9596–9605. <https://doi.org/10.1021/ma048472b>
 47. Luo G-F, Chen W-H, Zhang X-Z (2020) 100th anniversary of macromolecular science viewpoint: poly(N-isopropylacrylamide)-based thermally responsive micelles. *ACS Macro Lett* 9:872–881. <https://doi.org/10.1021/acscapm.0c00348>
 48. Mukherji D, Marques CM, Kremer K (2020) Smart responsive polymers: fundamentals and design principles. *Annu Rev Condens-Matter Phys* 11:271–299. <https://doi.org/10.1146/annurev-conma-phys-031119-050618>
 49. Yong H, Sommer J-U (2022) Cononsolvency effect: when the hydrogen bonding between a polymer and a cosolvent matters. *Macromolecules* 55:11034–11050. <https://doi.org/10.1021/acs.macromol.2c01428>
 50. Bharadwaj S, Niebuur B-J, Nothdurft K, Richtering W, van der Vegt N, Papadakis CM (2022) Cononsolvency of thermoresponsive polymers: where we are now and where we are going. *Soft Matter* 18:2884–2909. <https://doi.org/10.1039/d2sm00146b>
 51. Müller M, Rieser T, Dubin PL, Lunkwitz K (1998) Effects of salt on the temperature and pressure responsive properties of poly(N-vinylisobutyramide) aqueous solutions. *Colloid Polym Sci* 276:529–533. <https://doi.org/10.1007/s003960050276>
 52. Serizawa T, Chen M-Q, Akashi M (1998) Graft copolymers having hydrophobic backbone and hydrophilic branches. XVIII. Poly(styrene) nanospheres with novel thermosensitive poly(N-vinylisobutyramide)s on their surfaces. *J Polym Sci, Part A: Polym Chem* 36:2581–2587. [https://doi.org/10.1002/\(sici\)1099-0518\(199810\)36:14%3c2581::aid-pola17%3e3.0.co;2-e](https://doi.org/10.1002/(sici)1099-0518(199810)36:14%3c2581::aid-pola17%3e3.0.co;2-e)
 53. Suwa K, Yamamoto K, Akashi M, Takano K, Tanaka N, Kunugi S (1998) Effects of salt on the temperature- and pressure-responsive properties of poly(N-vinylisobutyramide) aqueous solutions. *Colloid Polym Sci* 276:529–533. <https://doi.org/10.1007/s003960050276>
 54. Kishida A, Kikunaga Y, Akashi M (1999) Synthesis and functionality of poly(N-vinylalkylamide). X. A novel aqueous two-phase system based on thermosensitive polymers and dextran. *J Appl Polym Sci* 73:2545–2548. [https://doi.org/10.1002/\(SICI\)1097-4628\(19990923\)73:13%3c2545::AID-APP1%3e3.0.CO;2-1](https://doi.org/10.1002/(SICI)1097-4628(19990923)73:13%3c2545::AID-APP1%3e3.0.CO;2-1)
 55. Kunugi S, Tada T, Tanaka N, Yamamoto K, Akashi M (2002) Microcalorimetric study of aqueous solution of a thermoresponsive polymer, poly(N-vinylisobutyramide) (PNVIBA). *Polym J (Jpn)* 34:383–388. <https://doi.org/10.1295/polymj.34.383>
 56. Patra L, Messman JM, Toomey R (2013) On the nature of volume-phase transitions in photo-cross-linked poly(cyclopropylacrylamide) and poly(N-vinylisobutyramide) coatings. *Soft Matter* 9:4349–4356. <https://doi.org/10.1039/c3sm26962k>
 57. Kan K, Ajiro H (2018) Switchable thermal responsive interpenetrated polymer network gels of poly(N-vinylacetamide) and poly(N-vinylisobutyramide). *Chem Lett* 47:591–593. <https://doi.org/10.1246/cl.171191>
 58. Yoshida H, Furumai H, Ajiro H (2022) Preparation and characterization of thermoresponsive poly(N-vinylisobutyramide) microgels. *Langmuir* 38:5269–5274. <https://doi.org/10.1021/acs.langmuir.1c02676>
 59. Kunugi S, Tada T, Yamazaki Y, Yamamoto K, Akashi M (2000) Thermodynamic studies on coil–globule transitions of poly(N-vinylisobutyramide-co-vinylamine) in aqueous solutions. *Langmuir* 16:2042–2044. <https://doi.org/10.1021/la991041f>
 60. Yamamoto K, Serizawa T, Muraoka Y, Akashi M (2000) Synthesis and functionalities of poly(N-vinylalkylamide). XII.

- Synthesis and thermosensitive property of poly(vinylamine) copolymer prepared from poly(*N*-vinylformamide-co-*N*-vinylisobutyramide). *J Polym Sci, Part A: Polym Chem* 38:3674–3681. [https://doi.org/10.1002/1099-0518\(20001001\)38:19%3c3674::aid-pola210%3e3.0.co;2-n](https://doi.org/10.1002/1099-0518(20001001)38:19%3c3674::aid-pola210%3e3.0.co;2-n)
61. Yamamoto K, Serizawa T, Muraoka Y, Akashi M (2001) Synthesis and functionalities of poly(*N*-vinylalkylamide). 13. Synthesis and properties of thermal and pH stimuli-responsive poly(vinylamine) copolymers. *Macromolecules* 34:8014–8020. <https://doi.org/10.1021/ma0102969>
 62. Chen C-W, Tano D, Akashi M (1999) Synthesis of platinum colloids sterically stabilized by poly(*N*-vinylformamide) or poly(*N*-vinylalkylamide) and their stability towards salt. *Colloid Polym Sci* 277:488–493. <https://doi.org/10.1007/s003960050414>
 63. Chen C-W, Takezako T, Yamamoto K, Serizawa T, Akashi M (2000) Poly(*N*-vinylisobutyramide)-stabilized platinum nanoparticles: synthesis and temperature-responsive behavior in aqueous solution. *Coll Surf A* 169:107–116. [https://doi.org/10.1016/S0927-7757\(00\)00422-2](https://doi.org/10.1016/S0927-7757(00)00422-2)
 64. Ito S (1989) Phase transition of aqueous solutions of poly(*N*-alkylacrylamide) derivatives. Effects of side chain structure. *Kobunshi Ronbunshu* 46:437–443. <https://doi.org/10.1295/koron.46.437>
 65. Tiktopulo EI, Uversky VN, Lushchik VB, Klenin SI, Bychkova VE, Ptitsyn OB (1995) “Domain” coil-globule transition in homopolymers. *Macromolecules* 28:7519–7524. <https://doi.org/10.1021/ma00126a032>
 66. Djokpé E, Vogt W (2001) *N*-Isopropylacrylamide and *N*-isopropylmethacrylamide: cloud points of mixtures and copolymers. *Macromol Chem Phys* 202:750–757. [https://doi.org/10.1002/1521-3935\(20010301\)202:5%3c750::AID-MACP750%3e3.0.CO;2-8](https://doi.org/10.1002/1521-3935(20010301)202:5%3c750::AID-MACP750%3e3.0.CO;2-8)
 67. Berndt I, Richtering W (2003) Doubly temperature sensitive core-shell microgels. *Macromolecules* 36:8780–8785. <https://doi.org/10.1021/ma034771+>
 68. Vishnevetskaya NS, Hildebrand V, Niebuur B-J, Grillo I, Filippov SK, Laschewsky A, Müller-Buschbaum P, Papadakis CM (2017) “Schizophrenic” micelles from doubly thermoresponsive polysulfobetaine-*b*-poly(*N*-isopropylmethacrylamide) diblock copolymers. *Macromolecules* 50:3985–3999. <https://doi.org/10.1021/acs.macromol.7b00356>
 69. Ko C-H, Claude K-L, Niebuur B-J, Jung FA, Kang J-J, Schanzenbach D, Frielinghaus H, Barnsley LC, Wu B, Pipich V, Schulte A, Müller-Buschbaum P, Laschewsky A, Papadakis CM (2020) Temperature-dependent phase behavior of the thermoresponsive polymer poly(*N*-isopropylmethacrylamide) in an aqueous solution. *Macromolecules* 53:6816–6827. <https://doi.org/10.1021/acs.macromol.0c01256>
 70. Kubota K, Hamano K, Kuwahara N, Fujishige S, Ando I (1990) Characterization of poly(*N*-isopropylmethacrylamide) in water. *Polym J (Jpn)* 22:1051–1057. <https://doi.org/10.1295/polymj.22.1051>
 71. Dybal J, Trchová M, Schmidt P (2009) The role of water in structural changes of poly(*N*-isopropylacrylamide) and poly(*N*-isopropylmethacrylamide) studied by FTIR, Raman spectroscopy and quantum chemical calculations. *Vibr Spectrosc* 51:44–51. <https://doi.org/10.1016/j.vibspec.2008.10.003>
 72. Kano M, Kokufuta E (2009) On the temperature-responsive polymers and gels based on *N*-propylacrylamides and *N*-propylmethacrylamides. *Langmuir* 25:8649–8655. <https://doi.org/10.1021/la804286j>
 73. Pang J, Yang H, Ma J, Cheng R (2011) Understanding different LCST levels of poly(*N*-alkylacrylamide)s by molecular dynamics simulations and quantum mechanics calculations. *J Theor Comp Chem* 10:359–370. <https://doi.org/10.1142/s0219633611006505>
 74. Kokufuta MK, Sato S, Kokufuta E (2012) LCST behavior of copolymers of *N*-isopropylacrylamide and *N*-isopropylmethacrylamide in water. *Colloid Polym Sci* 290:1671–1681. <https://doi.org/10.1007/s00396-012-2706-y>
 75. Ortiz de Solorzano I, Bejagam KK, An Y, Singh SK, Deshmukh SA (2020) Solvation dynamics of *N*-substituted acrylamide polymers and the importance for phase transition behavior. *Soft Matter* 16:1582–1593. <https://doi.org/10.1039/c9sm01798d>
 76. Netopilík M, Bohdanecký M, Chytrý V, Ulbrich K (1997) Cloud point of poly(*N*-isopropylmethacrylamide) solutions in water: is it really a point? *Macromol Rapid Commun* 18:107–111. <https://doi.org/10.1002/marc.1997.030180206>
 77. Kreuzer LP, Lindenmeir C, Geiger C, Widmann T, Hildebrand V, Laschewsky A, Papadakis CM, Müller-Buschbaum P (2021) Poly(sulfobetaine) versus poly(*N*-isopropylmethacrylamide): co-nonsolvency-type behavior of thin films in a water/methanol atmosphere. *Macromolecules* 54:1548–1556. <https://doi.org/10.1021/acs.macromol.0c02281>
 78. Alenichev I, Sedláková Z, Ilavský M (2007) Swelling and mechanical behavior of charged poly(*N*-isopropylmethacrylamide) and poly(*N*-isopropylacrylamide) networks in water/ethanol mixtures. Cononsolvency effect *Polym Bull* 58:191–199. <https://doi.org/10.1007/s00289-006-0586-3>
 79. Kouřilová H, Hanyková L, Spěváček J (2009) NMR study of phase separation in D₂O/ethanol solutions of poly(*N*-isopropylmethacrylamide) induced by solvent composition and temperature. *Eur Polym J* 45:2935–2941. <https://doi.org/10.1016/j.eurpolymj.2009.06.011>
 80. Wang P, Geiger C, Kreuzer LP, Widmann T, Reitenbach J, Liang S, Cubitt R, Henschel C, Laschewsky A, Papadakis CM, Müller-Buschbaum P (2022) Poly(sulfobetaine)-based diblock copolymer thin films in water/acetone atmosphere: modulation of water hydration and co-nonsolvency-triggered film contraction. *Langmuir* 38:6934–6948. <https://doi.org/10.1021/acs.langmuir.2c00451>
 81. Tu S, Zhang C (2015) Facile preparation of *N*-vinylisobutyramide and *N*-vinyl-2-pyrrolidinone. *Org Process Res Dev* 19:2045–2049. <https://doi.org/10.1021/acs.oprd.5b00303>
 82. Zhang J, Wang Z, Lin W, Chen S (2014) Gene transfection in complex media using PCBMAEE-PCBMA copolymer with both hydrolytic and zwitterionic blocks. *Biomater* 35:7909–7918. <https://doi.org/10.1016/j.biomaterials.2014.05.066>
 83. Suwa K, Wada Y, Kikunaga Y, Morishita K, Kishida A, Akashi M (1997) Synthesis and functionalities of poly(*N*-vinylalkylamide). IV. Synthesis and free radical polymerization of *N*-vinylisobutyramide and thermosensitive properties of the polymer. *J Polym Sci, Part A: Polym Chem* 35:1763–1768. [https://doi.org/10.1002/\(SICI\)1099-0518\(19970715\)35:9%3c1763::AID-POLA17%3e3.0.CO;2-3](https://doi.org/10.1002/(SICI)1099-0518(19970715)35:9%3c1763::AID-POLA17%3e3.0.CO;2-3)
 84. Akashi M, Nakano S, Kishida A (1996) Synthesis of poly(*N*-vinylisobutyramide) from poly(*N*-vinylacetamide) and its thermosensitive property. *J Polym Sci, Part A: Polym Chem* 34:301–303. [https://doi.org/10.1002/\(sici\)1099-0518\(19960130\)34:2%3c301::aid-pola16%3e3.0.co;2-u](https://doi.org/10.1002/(sici)1099-0518(19960130)34:2%3c301::aid-pola16%3e3.0.co;2-u)
 85. Chua PC, Kelland MA, Ajiro H, Sugihara F, Akashi M (2013) Poly(vinylalkanamide)s as kinetic hydrate inhibitors: comparison of poly(*N*-vinylisobutyramide) with poly(*N*-isopropylacrylamide). *Energy Fuels* 27:183–188. <https://doi.org/10.1021/ef301703w>
 86. Benaglia M, Chiefari J, Chong YK, Moad G, Rizzardo E, Thang SH (2009) Universal (switchable) RAFT agents. *J Am Chem Soc* 131:6914–6915. <https://doi.org/10.1021/ja901955n>
 87. Yoshioka M, Otsu T (1992) Reactivity of primary radicals in the radical polymerization of dialkyl fumarates initiated with dimethyl 2,2'-azobis(isobutyrate) and 2,2'-azobis(isobutyronitrile). *Macromolecules* 25:2599–2602. <https://doi.org/10.1021/ma00036a006>

88. Sato T, Shimooka S, Seno M, Tanaka H (1995) Radical polymerization behavior of ethyl ortho-formylphenyl fumarate involving intramolecular hydrogen abstraction. *J Polym Sci, Part A: Polym Chem* 33:2865–2873. <https://doi.org/10.1002/pola.1995.080331702>
89. Cochin D, Laschewsky A, Pantoustier N (2000) New substituted polymethylenes by free radical polymerization of bulky fumarates and their properties. *Polymer* 41:3895–3903. [https://doi.org/10.1016/S0032-3861\(99\)00650-3](https://doi.org/10.1016/S0032-3861(99)00650-3)
90. Keddie DJ, Moad G, Rizzardo E, Thang SH (2012) RAFT agent design and synthesis. *Macromolecules* 45:5321–5342. <https://doi.org/10.1021/ma300410v>
91. Ruiz-Rubio L, Vilas JL, Rodríguez M, León LM (2014) Thermal behaviour of H-bonded interpolymer complexes based on polymers with acrylamide or lactame groups and poly(acrylic acid): influence of N-alkyl and α -methyl substitutions. *Polym Degrad Stab* 109:147–153. <https://doi.org/10.1016/j.polymdegradstab.2014.07.012>
92. Li J-J, Zhou Y-N, Luo Z-H (2014) Thermal-responsive block copolymers for surface with reversible switchable wettability. *Ind Eng Chem Res* 53:18112–18120. <https://doi.org/10.1021/ie503610n>
93. Nuopponen M, Kalliomäki K, Laukkanen A, Hietala S, Tenhu H (2008) A-B-A stereoblock copolymers of *N*-isopropylacrylamide. *J Polym Sci, Part A: Polym Chem* 46:38–46. <https://doi.org/10.1002/pola.22355>
94. Biswas CS, Patel VK, Vishwakarma NK, Tiwari VK, Maiti B, Maiti P, Kamigaito M, Okamoto Y, Ray B (2011) Effects of tacticity and molecular weight of poly(*N*-isopropylacrylamide) on its glass transition temperature. *Macromolecules* 44:5822–5824. <https://doi.org/10.1021/ma200735k>
95. Suito Y, Isobe Y, Habaue S, Okamoto Y (2002) Isotactic-specific radical polymerization of methacrylamides in the presence of Lewis acids. *J Polym Sci, Part A: Polym Chem* 40:2496–2500. <https://doi.org/10.1002/pola.10337>
96. Isobe Y, Suito Y, Habaue S, Okamoto Y (2003) Stereocontrol during the free-radical polymerization of methacrylamides in the presence of Lewis acids. *J Polym Sci, Part A: Polym Chem* 41:1027–1033. <https://doi.org/10.1002/pola.10647>
97. Liu G, Zhou W, Zhang J, Zhao P (2012) Polymeric temperature and pH fluorescent sensor synthesized by reversible addition-fragmentation chain transfer polymerization. *J Polym Sci, Part A: Polym Chem* 50:2219–2226. <https://doi.org/10.1002/pola.25995>
98. Kouřilová H, Spěváček J, Hanyková L (2013) ¹H NMR study of temperature-induced phase transitions in aqueous solutions of poly(*N*-isopropylmethacrylamide)/poly(*N*-vinylcaprolactam) mixtures. *Polym Bull* 70:221–235. <https://doi.org/10.1007/s00289-012-0831-x>
99. Ding Z, Wang C, Feng G, Zhang X (2018) Thermo-responsive fluorescent polymers with diverse LCSTs for ratiometric temperature sensing through FRET. *Polymers* 10(283):281–210. <https://doi.org/10.3390/polym10030283>
100. Ree LHS, Opsahl E, Kelland MA (2019) *N*-Alkyl methacrylamide polymers as high performing kinetic hydrate inhibitors. *Energy Fuels* 33:4190–4201. <https://doi.org/10.1021/acs.energyfuels.9b00573>
101. Reitenbach J, Geiger C, Wang P, Vagias A, Cubitt R, Schanzenbach D, Laschewsky A, Papadakis CM, Müller-Buschbaum P (2023) Effect of magnesium salts with chaotropic anions on the swelling behavior of PNIPMAM thin films. *Macromolecules* 56:567–577. <https://doi.org/10.1021/acs.macromol.2c02282>
102. Ruiz-Rubio L, Álvarez V, Lizundia E, Vilas JL, Rodríguez M, León LM (2015) Influence of α -methyl substitutions on interpolymer complexes formation between poly(meth)acrylic acids and poly(*N*-isopropyl(meth)acrylamide)s. *Colloid Polym Sci* 293:1447–1455. <https://doi.org/10.1007/s00396-015-3529-4>
103. Brugnoli M, Nickel AC, Kröger LC, Scotti A, Pich A, Leonhard K, Richtering W (2019) Synthesis and structure of deuterated ultra-low cross-linked poly(*N*-isopropylacrylamide) microgels. *Polym Chem* 10:2397–2405. <https://doi.org/10.1039/C8PY01699B>
104. Habaue S, Isobe Y, Okamoto Y (2002) Stereocontrolled radical polymerization of acrylamides and methacrylamides using Lewis acids. *Tetrahedron* 58:8205–8209. [https://doi.org/10.1016/S0040-4020\(02\)00969-9](https://doi.org/10.1016/S0040-4020(02)00969-9)
105. Zhang J, Liu W, Nakano T, Okamoto Y (2000) Stereospecific radical polymerization of *N*-methyl methacrylamide. *Polym J (Jpn)* 32:694–699. <https://doi.org/10.1295/polymj.32.694>
106. Salmerón Sánchez M, Hanyková L, Ilavský M, Monleón Pradas M (2004) Thermal transitions of poly(*N*-isopropylmethacrylamide) in aqueous solutions. *Polymer* 45:4087–4094. <https://doi.org/10.1016/j.polymer.2004.04.020>
107. Meeussen F, Nies E, Berghmans H, Verbrugge S, Goethals E, Du Prez F (2000) Phase behaviour of poly(*N*-vinyl caprolactam) in water. *Polymer* 41:8597–8602. [https://doi.org/10.1016/s0032-3861\(00\)00255-x](https://doi.org/10.1016/s0032-3861(00)00255-x)
108. Lessard DG, Ousalem M, Zhu XX (2001) Effect of the molecular weight on the lower critical solution temperature of poly(*N*, *N*-diethylacrylamide) in aqueous solutions. *Can J Chem* 79:1870–1874. <https://doi.org/10.1139/v01-180>
109. Miasnikova A, Laschewsky A (2012) Influencing the phase transition temperature of poly(methoxy diethylene glycol acrylate) by molar mass, end groups, and polymer architecture. *J Polym Sci, Part A: Polym Chem* 50:3313–3323. <https://doi.org/10.1002/pola.26116>
110. Hechenbichler M, Laschewsky A, Gradzielski M (2021) Poly(*N*, *N*-bis(2-methoxyethyl)acrylamide), a thermoresponsive non-ionic polymer combining the amide and the ethyleneglycol ether motifs. *Colloid Polym Sci* 299:205–219. <https://doi.org/10.1007/s00396-020-04701-9>
111. Hirano T, Kamikubo T, Okumura Y, Sato T (2007) Heterotactic poly(*N*-isopropylacrylamide) prepared via radical polymerization in the presence of fluorinated alcohols. *Polymer* 48:4921–4925. <https://doi.org/10.1016/j.polymer.2007.06.059>
112. Amiya T, Hirokawa Y, Hirose Y, Li Y, Tanaka T (1987) Reentrant phase transition of *N*-isopropylacrylamide gels in mixed solvents. *J Chem Phys* 86:2375–2379. <https://doi.org/10.1063/1.452740>
113. Winnik FM, Ringsdorf H, Venzmer J (1990) Methanol-water as a co-nonsolvent system for poly(*N*-isopropylacrylamide). *Macromolecules* 23:2415–2416. <https://doi.org/10.1021/ma00210a048>
114. Scherzinger C, Schwarz A, Bardow A, Leonhard K, Richtering W (2014) Conosolvency of poly-*N*-isopropyl acrylamide (PNIPAM): microgels versus linear chains and macrogels. *Curr Opin Coll Interface Sci* 19:84–94. <https://doi.org/10.1016/j.cocis.2014.30.011>
115. Kyriakos K, Philipp M, Lin C-H, Dyakonova M, Vishnevetskaya N, Grillo I, Zaccone A, Miasnikova A, Laschewsky A, Müller-Buschbaum P, Papadakis CM (2016) Quantifying the interactions in the aggregation of thermoresponsive polymers: the effect of conosolvency. *Macromol Rapid Commun* 37:420–425. <https://doi.org/10.1002/marc.201500583>
116. Xue N, Qiu X-P, Aseyev V, Winnik FM (2017) Nonequilibrium liquid-liquid phase separation of poly(*N*-isopropylacrylamide) in water/methanol mixtures. *Macromolecules* 50:4446–4453. <https://doi.org/10.1021/acs.macromol.7b00407>
117. Raftopoulos KN, Kyriakos K, Nuber M, Niebuur B-J, Holderer O, Ohl M, Ivanova O, Pasini S, Papadakis CM (2020) Co-nosolvency in concentrated aqueous solutions of PNIPAM: effect of methanol on the collective and the chain dynamics. *Soft Matter* 16:8462–8472. <https://doi.org/10.1039/d0sm01007c>
118. Ko C-H, Henschel C, Meledam GP, Schroer MA, Guo R, Gaetani L, Müller-Buschbaum P, Laschewsky A, Papadakis CM (2021) Co-nosolvency effect in solutions of poly(methyl methacrylate)-*b*-poly(*N*-isopropylacrylamide) diblock copolymers in water/

- methanol mixtures. *Macromolecules* 54:5825–5837. <https://doi.org/10.1021/acs.macromol.1c00512>
119. Niebuur B-J, Lohstroh W, Ko C-H, Appavou M-S, Schulte A, Papadakis CM (2021) Pressure dependence of water dynamics in concentrated aqueous poly(*N*-isopropylacrylamide) solutions with a methanol cosolvent. *Macromolecules* 54:4387–4400. <https://doi.org/10.1021/acs.macromol.1c00111>
120. Niebuur B-J, Deyerling A, Höfer N, Schulte A, Papadakis CM (2022) Cononsolvency of the responsive polymer poly(*N*-isopropylacrylamide) in water/methanol mixtures: a dynamic light scattering study of the effect of pressure on the collective dynamics. *Colloid Polym Sci* 300:1269–1279. <https://doi.org/10.1007/s00396-022-04987-x>
121. Costa ROR, Freitas RFS (2002) Phase behavior of poly(*N*-isopropylacrylamide) in binary aqueous solutions. *Polymer* 43:5879–5885. [https://doi.org/10.1016/S0032-3861\(02\)00507-4](https://doi.org/10.1016/S0032-3861(02)00507-4)
122. Schild HG, Muthukumar M, Tirrell DA (1991) Cononsolvency in mixed aqueous solutions of poly(*N*-isopropylacrylamide). *Macromolecules* 4:948–952. <https://doi.org/10.1021/ma00004a022>
123. Mukae K, Sakurai M, Sawamura S, Makino K, Kim SW, Ueda I, Shirahama K (1994) Swelling of poly(*N*-isopropylacrylamide) gels in water-aprotic solvent mixtures. *Colloid Polym Sci* 272:655–663. <https://doi.org/10.1007/bf00659279>
124. Bharadwaj S, van der Vegt NFA (2019) Does Preferential adsorption drive cononsolvency? *Macromolecules* 52:4131–4138. <https://doi.org/10.1021/acs.macromol.9b00575>
125. Mukherji D, Marques CM, Kremer K (2014) Polymer collapse in miscible good solvents is a generic phenomenon driven by preferential adsorption. *Nat Commun* 5(4882):4881–4886. <https://doi.org/10.1038/ncomms5882>
126. Hore MJA, Hammouda B, Li Y, Cheng H (2013) Co-nonsolvency of poly(*N*-isopropylacrylamide) in deuterated water/ethanol mixtures. *Macromolecules* 46:7894–7901. <https://doi.org/10.1021/ma401665h>
127. Yamauchi H, Maeda Y (2007) Co-nonsolvency effect of thermo-sensitive *N*-isopropylacrylamide nanometer-sized gel particles in water–PEG systems. *J Phys Chem* 111:12964–12968. <https://doi.org/10.1021/jp072438s>
128. Pagonis K, Bokias G (2006) Simultaneous lower and upper critical solution temperature-type co-nonsolvency behaviour exhibited in water–dioxane mixtures by linear copolymers and hydrogels containing *N*-isopropylacrylamide and *N*, *N*-dimethylacrylamide. *Polym Int* 55:1254–1258. <https://doi.org/10.1002/pi.2072>
129. Cameron NS, Corbierre MK, Eisenberg A (1999) Asymmetric amphiphilic block copolymers in solution: a morphological wonderland. *Can J Chem* 77:1311–1326. <https://doi.org/10.1139/v99-141>
130. Bivigou-Koumba AM, Kristen J, Laschewsky A, Müller-Buschbaum P, Papadakis CM (2009) Synthesis of symmetrical triblock copolymers of styrene and *N*-isopropylacrylamide using bifunctional bis(trithiocarbonate)s as RAFT agents. *Macromol Chem Phys* 210:565–578. <https://doi.org/10.1002/macp.200800575>
131. Yong H, Merlitz H, Fery A, Sommer J-U (2020) Polymer brushes and gels in competing solvents: the role of different interactions and quantitative predictions for poly(*N*-isopropylacrylamide) in alcohol–water mixtures. *Macromolecules* 53:2323–2335. <https://doi.org/10.1021/acs.macromol.0c00033>
132. Grinberg VY, Burova TV, Grinberg NV, Moskalets AP, Dubovik AS, Plashchina IG, Khokhlov AR (2020) Energetics and mechanisms of poly(*N*-isopropylacrylamide) phase transitions in water–methanol solutions. *Macromolecules* 53:10765–10772. <https://doi.org/10.1021/acs.macromol.0c02253>

Publisher's Note Springer Nature remains neutral with regard to jurisdictional claims in published maps and institutional affiliations.